LIGAND EXCHANGE PHOTOCHEMISTRY OF IODOPENTAAMMINERHODIUM (III) IN A SODIUM/HYDROGEN Y TYPE ZEOLITE

A Thesis

by

MICHAEL JOSEPH CAMARA

Submitted to the Graduate College of
Texas A&M University
in partial fulfillment of the requirement for the degree of

MASTER OF SCIENCE

May 1981

Major Subject: Chemistry

LIGAND EXCHANGE PHOTOCHEMISTRY OF IODOPENTAAMMINERHODIUM (III)

IN A SODIUM/HYDROGEN Y TYPE ZEOLITE

A Thesis

by

MICHAEL JOSEPH CAMARA

Approved as to style and content by:

(Chairman of Committee)

(Member)

(Member)

(Head of Department)

May 1981

ABSTRACT

Ligand Exchange Photochemistry of Iodopentaamminerhodium(III) in a Sodium/Hydrogen Y Type Zeolite (May 1981)

Michael Joseph Camara, B. S., Fordham University

Chairman of Advisory Committee: Dr. Jack H. Lunsford

The photoaquation of iodopentaamminerhodium(III) supported in a hydrated Y-type zeolite was observed and the quantum efficiency of this reaction has been determined to be 0.26±0.06 at 435 nm. Partial dehydration of the zeolite resulted in a lower value for the quantum yield of 0.20±0.07. The ammonia produced by this reaction was trapped within the zeolite as ammonium ions and semi-quantitatively analyzed by infrared spectroscopy.

The rate was observed to fall off after ~50 min due to the depletion of reactant and/or the attenuation of the light due to absorption by the product and scattering by the support. Determination of light scattered by the solid support represented the largest single source of error. Several theories are reviewed and applied to account for the scattering. These include the theory of exponential attenuation of incident radiation, the Kubelka-Monk theory, and a particle model theory. Approximations had to be made in every case in order to apply the resulting complex equations to the experimentally observable parameters.

Reflectance spectroscopy provided an essentially independent way to determine the quantum yield; the change in the reflectance was small enough for the rate to be adequately described by the Kubelka-Monk and particle model theories.

ACKNOWLEDGEMENTS

The author wishes to express his appreciation to Dr. Jack H. Lunsford for the opportunity to study under him and for his guidance and support. The author also wishes to acknowledge the following people for their friendship as well as for their theoretical and experimental insight: Bruce Gustafson, Francois Fajula, William Quayle, and John Pearce.

DEDICATION

This work is dedicated to

my mother and father

TABLE OF CONTENTS

LIST OF TABLES

LIST OF FIGURES

INTRODUCTION

Reports of chemical storage of solar (visible light) energy are becoming increasingly prevalent.[1] The splitting of water into hydrogen and oxygen using photoactive catalysts,[2-5] for example, offers the advantages of a plentiful raw material as well as a product with a high energy-to-mass ratio.[6] The catalytic behavior of zeolites is well known,[7,8] thus an inquiry into the likelihood of their use in photocatalytic systems is a natural extension of current research. In our laboratories initial investigations into the preparation and characterization of potentially photoactive (heterogeneous) catalysts have been undertaken. Underlying these investigations is the prospect that a catalyst able to chemically store (sun-) light energy may be developed, to ease, if not eliminate, the current energy shortage problem.

The first topic to be considered is the photo-behavior of the support, namely the Y-type zeolite. The photo-behavior of the support includes the extent to which it absorbs or scatters light, thus preventing photons from reaching the active site, as well as its effect on the relaxation and/or reaction of the chromophore contained in this relatively rigid system. Thus, in order to determine the effects that the zeolite may have upon a photochemical reaction, iodopentaammine-rhodium (III) perchlorate has been prepared and its subsequent photoaquation has been studied in solution as well as in the zeolite. A

This thesis follows the style and format of the Journal of Physical Chemistry.

comparison of the results obtained reflects the different influences exerted by the two media.

The photochemistry of liquid solutions has been studied much more extensively than that of solids[9] for several reasons. Light scattering by a solid is a problem which does not exist in solution. Furthermore, when the nature of the solid serves to limit diffusion of reactants and products, the relatively rapid buildup of product at, or very near the surface could limit further reaction in the bulk. This is true especially if product diffusion is limited and the products absorb significantly in the region of the exciting frequency. The latter is known as the internal filtering effect. Obviously, quantitative evaluation of photophysical and photochemical processes, in this case quantum yield, will require special mathematical treatments.

When transition metal complexes are irradiated in the visible or ultraviolet region, three types of excitation are possible. At high energies charge transfer occurs which is the actual movement of an electron from the ligands to the central metal ion or vice versa. Also found at relatively high energies are internal ligand transitions which involve only excitation of the ligand molecular orbital system. This type of transition involves a change in electron density of the ligand system. At lower energies ligand field transitions occur; that is, excitation of the electrons in the d-orbitals of the metal. This causes a change in the electron density between the metal and the ligand and is primarily responsible for ligand exchange reactions. In the present study we are concerned with this last case.

The choice of iodopentaamminerhodium (III) as a probe came as the result of a consideration of the properties of the Y-type zeolite and the desired wavelength of the exciting energy (i.e., visible light). The sodium form of the Y-type zeolite is basic in character. Of the transition metals considered initially, ammine rather than aquo complexes were chosen in order to avoid the possibility of polymeric hydroxide formation. In the absence of these polymeric hydroxides the cationic complexes exchange into the zeolite readily.

References concerning the photochemical behavior of chromium (III) complexes in solution constitute a large fraction of the present transition metal photochemical literature.[10,10a] In the visible region, the photoaquation of $Cr(NH_3)_5X^{2+}$ ($X = Cl^-$, Br^-) occurs[11,12] with moderate quantum yields of ammonia, $\phi_{NH_3} \leq 0.38$. The quantum yield, ϕ, of a reaction can be defined as the ratio of the number of molecules reacted to the number of photons absorbed by the reactant. The molar extinction coefficient, ε, in each of the above cases is less than 50 $M^{-1}cm^{-1}$. The reciprocal of the molar extinction coefficient represents the molar concentration necessary for 90% absorption of the incident light at a given wavelength as it traverses a 1 cm path-length. When other conditions are the same, larger values of ϕ and ε are desirable since they will insure larger amounts of product formation in a given amount of time.

Ligand field (LF) excitation of $Co(NH_3)_5X^{2+}$, ($X = Cl^-$, Br^-, I^-)[13,14] results in anion aquation; the quantum yield in these cases is less than 0.01 (ϕ_{aq}). The molar extinction coefficients of these cobalt

complexes in the spectral region of LF excitation are always less than or equal to 80 $M^{-1}cm^{-1}$.

For the complexes of the type $Rh(NH_3)_5X^{2+}$, (X = Cl^-, Br^-, I^-) only the bromide and iodide complexes absorb in the visible region.[15] The bromide complex, however, exhibits both a relatively small quantum yield for ammine aquation[16] (ϕ_{NH_3} = 0.17) and a very small molar extinction coefficient (ε = 25 $M^{-1}cm^{-1}$). For the iodide complex the quantum yield is large[17] (ϕ_{NH_3} = 0.87), and the molar extinction coefficient of the ligand field transition is also of a respectable magnitude (ε_{max} = 270 M^{-1} cm^{-1}).[15]

This reaction when performed in dilute acid proceeds as follows:

$$Rh(NH_3)_5I^{2+} + H_3O^+ \xrightarrow{h\nu} Rh(NH_3)_4OH_2I^{2+} + NH_4^+ \qquad (1)$$

The trans- form of the complex is produced almost exclusively. The quantum yield for the most noticeable side product ($Rh(NH_3)_4I_2^+$) is less than 10^{-3}. The dilute acid in which this reaction is performed serves to trap the ammonia photoproduct as the ammonium ion. The trans iodoaquo product does not have an absorption maximum at the exciting frequency, but its broad d-d transition band does significantly overlap with that of the reactant. This results in a decrease in the apparent quantum yield as the concentration of product becomes significant.

Theory

A mole of photons is called an einstein (E). For a simple reaction:

$$C \xrightarrow{h\nu} P \tag{2}$$

where C is the reactant and P is the product, the quantum yield can be defined as:

$$\phi = \frac{\text{moles of product formed}}{\text{moles of photons absorbed}} \tag{3}$$

The denominator represents light absorbed by the reactant. When the intensity of the light source, I_o (in $E \cdot cm^{-2} \cdot min^{-1}$) is small; i.e., when short periods of irradiation have a negligible effect on the concentration of reactant, then the reaction will be zero order. Assuming all the incident radiation is absorbed, the rate equation may be written as follows:

$$\frac{dP}{dt} = \phi I_o \tag{4}$$

As the irradiation time goes from zero to time, t, the concentration of product will increase from zero to [P]. This is represented mathematically by:

$$\int_0^P dP = \phi I_o \int_0^t dt \tag{5}$$

Performing the required integration yields:

$$P = \phi I_o t \tag{6}$$

A plot of moles of product formed versus time should yield a straight line. If the intensity of the source is known, then the quantum yield can be calculated. Conversely, values of P/t should be constant, thus as any time t:

$$\phi = \frac{P}{I_o t} \tag{7}$$

In reality only a fraction of the incident radiation (f_{abs}) is absorbed, thus eq 6 must be rewritten as follows:

$$P = \phi f_{abs} I_o t \tag{8}$$

The method used to determine f_{abs} can result in more complicated equations since it also depends on light absorption by the photoproducts at the exciting wavelength (and/or other reactants, if present) and the physical state of the photolyte. If the photolyte is a solid, then f_{abs} depends on the nature of the material, i.e., (a) whether it is a supported adsorbate or a pure solid, and (b) whether the solid surface is continuous or particulate in nature. Finally, in very precise analytical work, the extent to which the glass or other container absorbs or reflects the light, thus preventing it from reaching the photolyte, will also influence f_{abs}.[18] This last problem presents a relatively small correction and will not be dealt with further.

The determination of quantum yields in solution is readily understood and methods can be found in standard textbooks on photochemistry.[18-20] The derivation is relatively straightforward.

The transmission of a solution, T, is defined as follows:

$$T = \frac{I}{I_o} = 10^{-\varepsilon[c]\ell} \tag{9}$$

where I is the intensity of the light emerging from the sample 180° from the angle of incidence through a cell of thickness, ℓ, containing a solution of concentration [c]. The molar extinction coefficient (ε) is dependent on the chemical composition of the absorber as well as the illuminating frequency. The fraction of light absorbed is equal to that which is not transmitted, or:

$$f_{abs} = 1-(I/I_o) \tag{10}$$

Combining eq 9 and 10 yields:

$$f_{abs} = 1-10^{-\varepsilon[c]\ell} \tag{11}$$

If the incident intensity, I_o, is expressed in units of $E \cdot min^{-1} \cdot Liter^{-1}$, then eq 8 and 11 can be combined to give:

$$[P] = \phi I_c(1-10^{-\varepsilon[c]\ell})t \tag{12}$$

where [P] is the molar concentration of P and I_c represents the source intensity in units of $E \cdot Liter^{-1} min^{-1}$. If only one reactant absorbs radiation and if the concentration of reactant at any time, t, is much greater than the product, then any possible interferences by the product will be small and can be ignored. The quantum yield is obtained by rearrangement of eq 12 as shown:

$$\phi = \frac{[P]}{I_c(1-10^{-\varepsilon[c]\ell})t} \tag{13}$$

It should be reemphasized that this is only strictly true for small conversion to product.

The photochemistry of the solid state has been divided into two classes. The first deals with reactions of pure solids or homogeneous mixtures (e.g., solid solutions); the second deals with reactions of species which are adsorbed on a support. The most common problems of solid state photochemistry, which include light scattering, reflection, and concentration gradients (due to reactant/product immobility), can become aggravated when the influence of diffusion is important and the evaluation of the actual surface concentration is dependent on the nature and concentration of active surface states.[21] These additional problems are primarily due to adsorption phenomena.

Several attempts have been made to choose conditions which would minimize or eliminate some of the problems mentioned above. This allowed each system to be handled more easily. For example, in dealing with the photochemistry of molecules in the adsorbed state, certain authors[22-24] used a porous vycor glass as the support to eliminate scattering. The glass was reported to have a good transmission down to 210 nm. Others have placed the adsorbant silica[25] or alumina[26] in a solvent of similar refractive index to minimize the scattering problem. Literature references for the latter case, however, are few in number when compared with the wealth of information concerning the photochemistry of pure solids.

Much of the recent work on pure solids makes use of reflectance or a combination of reflectance and transmittance measurements of

reactants (and products).[27-35] The strength or weakness of each method rests on the validity of the mathematical derivation of f_{abs}, the fraction of light absorbed by the reactant. The reactant concentration must be taken into consideration if it is small since relatively small amounts of exposure could cause large changes in concentration. This is often the case with very thin films.[27,28,36] Relatively rapid reactions (on the order of minutes) and highly reflective solids (where "local" rate equations must be employed) are other examples where the reactant concentration is important.[37,38] These last two have only been treated theoretically.

A method has also been developed for determining the quantum yield of a reaction at relatively large conversion.[39,40] In nearly every case, simplifying assumptions are necessary in order to find solutions to the complex theoretical equations.

At present, infrared spectroscopy has received little attention as a tool for the quantitative determination of reactants and/or products leading to quantum yield determinations.[41,42] The sensitivity of infrared is often sufficient to detect very small concentrations of product.[43]

As previously stated, solid state photochemistry has been divided into two divisions; one deals with pure solids while the other deals with adsorbed species. In the past an examination of either of these has always excluded the other. The following methods combine solid state photochemistry and photochemistry of supported complexes by linking the theory of the former with the experimental design of the

latter. One method gives an approximate solution, whereas, the others provide more rigorous treatments.

Determination of Quantum Yield Using Infrared Spectroscopy

Pseudo zero order approximation. In the first of these methods an approximate quantum yield solution is obtained as follows. Assume that the wafer does not transmit visible light and that it is partially transparent to infrared. Further assume that only the reactant absorbs in the region of excitation and that the diffuse reflectance of the sample is the same over its entire (apparent) surface. In this case, where no visible light is transmitted, the incident light must be absorbed or reflected. The fraction of the light initially absorbed by the reactant is given by:

$$f_{abs} = 1 - R \tag{14}$$

where R is the measured reflectance of the sample. If the extent of reaction is small, ≤10%, then f_{abs} may be considered a constant and the rate equation is

$$\frac{d[P]}{dt} = \phi(1 - R)I_o \tag{15}$$

which can be integrated between the appropriate limits to give:

$$[P] = \phi(1 - R)I_o t \tag{16}$$

The symbol I_o used here signifies the light intensity in units of $E \cdot cm^{-2} \cdot min^{-1}$, and [P] is the number of moles of product per square

centimeter; [P], can be determined by its infrared absorption (assuming calibration curves have been previously prepared).

For small conversion with no internal filter effect, i.e., no absorption by species other than the reactant, the reflectance will be constant. If the light intensity, I_o, and the factor P/t are both constant (the latter will be constant if the reaction is zero order), then the quantum yield can be easily calculated from eq 16.

First order approximation. In a second and more rigorous treatment the rate of reaction of a thin layer of powder, originally described for a solid state (initially pure) system,[36] can be easily applied to the present system. Consider a thin layer (one particle deep) of reactant C in the form of spherical particles having a rough surface which reacts to give product P:

$$C + h\nu \longrightarrow P \tag{17}$$

The incident radiation ($h\nu$) is both monochromatic and perpendicular to the surface. In each particle there are N moles of C thus the rate of reaction may be described by:

$$\frac{dN}{dt} = -A\phi I\pi d^2/4 \tag{18}$$

Here A is the fraction of light absorbed by the reactant and $I\pi d^2/4$ is the number of Einsteins incident on the particle. The particle diameter is denoted by d. The concentration of C per unit area is given by:

$$[C] = mN/Z \tag{19}$$

where m is the number of particles, each containing N moles, and Z is the surface area. Combining eq 18 and 19 yields the rate equation in terms of concentration:

$$\frac{d[C]}{dt} = -mA\phi I\pi d^2/4Z \qquad (20)$$

The fraction of light absorbed (A) depends on several factors. In a previous derivation[29] two factors $\bar{m}_e$ and $\bar{m}_i$ are defined as the fraction of light which is reflected externally off a particle and internally off the inner boundary of the particle. These two factors are related to the refractive index of the material in question.

Of the light incident on a particle, $(1 - m_e)$ enters the particle. It has been found that the light travels a distance of 2d/3 before again encountering the particle surface. During this time a fraction, $(1 - a)$, of the light is absorbed by the particle and $(1 - a_c)$ is absorbed by the reactant. The factors a and a_c are defined for small conversion by the Lambert equation, as follows:

$$a = \exp[k_c N 2d/3N_o - k_p N_p 2d/3N_o] \qquad (21)$$

and

$$a_c = \exp[k_c N 2d/3N_o] \qquad (22)$$

The coefficients of absorption for reactant and product are k_c and k_p, respectively. The total number of moles of c initially present is indicated by N_o. The moles of product P (N_p) is given by

$$N_p = N_o - N \qquad (23)$$

At the end of one passage through the particle, the light reaches the inner surface. Part of this radiation, (m_i), is reflected back into the particle. An infinite number of such passes then ensue. The total fraction of light absorbed then is the sum of the light absorbed during each of these passes:

$$A = (1 - \bar{m}_e)[(1 - a_c) + \bar{m}_i a(1 - a_c) + \bar{m}_i{}^2 a^2(1 - a_c) + \cdots] \quad (24)$$

or

$$A = (1 - \bar{m}_e)(1 - a_c) \sum_{j=0}^{\infty} (\bar{m}_i a)^j \quad (25)$$

This equation converges to give:

$$A = (1 - \bar{m}_e)(1 - a_c)/(1 - \bar{m}_i a) \quad (26)$$

Equations 21, 22 and 26 can be combined to yield:

$$A = \frac{(1 - \bar{m}_e)[1 - \exp(-2k_c Nd/3N_o)]}{[1 - \bar{m}_i \exp(-2k_c Nd/3N_o - 2k_p N_p d/3N_o)]} \quad (27)$$

Equations 20 and 27 completely describe the system in question based on fundamental optical parameters.

A few simplifying assumptions will make the use of these equations somewhat more tractable. The rough surfaced spherical particle model is only valid for weak absorbers. In the case of a weak absorber, the radiation intensity striking each particle is also constant. For weakly absorbing layers, a and a_c are nearly unity. This will tend to simplify eq 27 since:

$$1 - \bar{m}_i a \cong 1 - \bar{m}_i \quad (28)$$

and

$$1 - a_c = 1 - \exp(-2k_c Nd/3N_o) \tag{29}$$

$$\cong 2k_c Nd/3N_o \tag{30}$$

After noting this, eq 27 may be rewritten:

$$A = (2k_c Nd/3N_o)(1 - \bar{m}_e)/(1 - \bar{m}_i) \tag{31}$$

It has previously been found[29] that:

$$\eta^2 = (1 - \bar{m}_e)/(1 - \bar{m}_i) \tag{32}$$

where η is the refractive index. Now eq 20, 31, and 32 can be combined to yield

$$d[C]/dt = -\phi I \pi d^3 k_c \eta^2 mN/6ZN_o \tag{33}$$

Equation 19 can be substituted into eq 33 and as a result:

$$d[C]/dt = -\phi I[C]\pi k_c d^3 \eta^2/6N_o \tag{34}$$

The number of moles of pure reactant initially present (N_o) is given by:

$$N_o = \rho \pi d/6M \tag{35}$$

where ρ is the density of C, M is the molecular weight and $\pi d^3/6$ is the volume of a sphere of diameter d. With this, eq 34 becomes:

$$d[C]/dt = -\phi I[C]k_c \eta^2 M/\rho \tag{36}$$

The molar absorption coefficient for solids, ε (in cm^2/mole), is defined by:

$$\varepsilon = k_c M/\rho \tag{37}$$

Finally, the rate equation may be obtained in experimetally applicable form by combining eq 36 and 37 to give:

$$d[C]/dt = -\phi\varepsilon\eta^2 I[C] \tag{38}$$

An assumption included in the derivation of eq 38 is that the refractive index η does not change with time, or that the indices of refraction of the reactant and product are very nearly the same.

Inner filter effect. Based on the observation that the photoproduct forms initially on the surface of a solid photolyte and the assumption that this photoproduct then attenuates part or all of the incident radiation reaching the remaining reactant, a semiempirical approach has been developed to describe this inner filter effect.[39] The derivation is as follows.

Consider a skin of photoproduct x cm thick which increases as irradiation proceeds. Since there must be an intermediate region where both reactant and product are present, the purity of this skin is open to some doubt. Therefore let x represent some average skin thickness such that if all the photoproduct were concentrated at the surface, its thickness would be x.

The assumption that the intensity I, transmitted through the photoproduct falls off exponentially as thickness increases is expressed mathematically by:

$$I = I_o e^{-kx} \tag{39}$$

The parameter k is called an attenuation constant and it represents the absorption coefficient of the product if the medium does not scatter light. If light scattering is important, then k represents a combination of absorption and scattering factors.

When the concentration of product [P] is measured in moles·cm^{-2} and the density of the solid (ρ) is in moles·cm^{-3} then the rate of reaction can be described by:

$$\frac{d[P]}{dt} = \frac{\rho dx}{dt} = \phi I = \phi I_o e^{-kx} \tag{40}$$

Within this equation are the assumptions that the wafer is infinitely thick (transmission = 0) and that the quantum yield is independent of wafer thickness.

Integration and rearrangement yields:

$$x = \frac{1}{k} \ln(1 + \frac{k\phi}{\rho} I_o t) \tag{41}$$

After defining a normalized attenuation constant, k', where k' = k/ρ, and converting x to [P], a two parameter equation emerges:

$$[P] = \frac{1}{k'} \ln(1 + k'\phi I_o t) \tag{42}$$

This equation then, relates the moles of incident photons·cm^{-2}, $I_o t$, to the moles of product·cm^{-2}, [P].

Determination of Quantum Yield by Reflectance Spectroscopy

The two derivations presented here are based on two widely accepted theories in diffuse reflectance spectroscopy: the Kubelka-Munk theory

and the particle model theory. A comparison between these and among other theories with regards to reflectance has already been published;[44] however, a brief discussion will help put the derivations in perspective.

The Kubelka-Munk theory treats a powdered sample as a continuous medium. Two empirical parameters are postulated to account for light scattering and absorption by the sample, but they do not represent any fundamental property of the sample. Despite the empirical nature of this theory, its widespread acceptance and long standing is indicative of its applicability and usefulness with regards to diffuse reflectance spectroscopy.

The particle model theory, as the name signifies, treats a powdered sample as a collection of spherical particles. As first introduced by Melamed,[45] this theory relates the reflective property of the powder to its index of refraction and absorption coefficient. Although more recent in its development, this theory draws its significance from the fact that it correctly describes reflectance spectroscopy and is able to relate the reflective property of the powder to fundamental optical parameters.

Continuous medium model. Although the Kubelka-Munk theory makes use of arbitrary constants that are not fundamental optical parameters, the equations that result allow for relatively easy handling of reflectance data and good comparison with experiment. The theory is as follows.[30]

Consider an infinitely thick solid. The change in the intensity (I) of the light as it moves into the solid with respect to the depth x into the solid is given by:

$$dI/dx = -(k' + s)I + sJ \tag{43}$$

where k' is the absorption coefficient of the solid (which is related to k, the absorption coefficient in Beers law) and s is the scattering coefficient of the solid. The change in the intensity (J) of light moving out of the solid is given by:

$$dJ/dx = (k' + s)J - sI \tag{44}$$

The absorption constant is the sum of the absorptions of the reactant and product

$$k' = \frac{C_A}{C_o} k'_A + \frac{C_P}{C_o} k'_P \tag{45}$$

where k'_A and k'_P are the absorption coefficients for pure A, and pure P respectively, C_o is the concentration of pure A at t = 0 and C_A and C_P are the concentrations of reactant and product at time t and distance x into the sample.

The local rate equation is then given by

$$dC_A/dt = k'_A \phi C_A/C_o (I + J) \tag{46}$$

where ϕ is the quantum yield.

For diffuse radiation it can be shown[27] that:

$$R = J/I \tag{47}$$

In the case of a reaction, eq 47 is only true for short reaction times. Equations 9, 10, and 12 can be solved (see appendix) to give:

$$f = (1 - R)^2/2R \cong k'/s \tag{48}$$

where f is called the remission function. Equations 46 and 47 can be combined to give:

$$dC_A/dt = -k'_A\phi(C_A/C_o)I_o(1 + R) \tag{49}$$

where I_o has replaced I since the reflectance can only be measured at the surface of the solid. The concentration of reactant may be obtained by combining eq 45 and 49, and realizing that $C_o = C_A + C_P$ to give:

$$C_A = \frac{sC_o}{k'_A - k'_P}\left[\frac{1 - R^2}{2R} - \frac{k'_P}{s}\right] \tag{50}$$

Equations 49 and 50 may be solved exactly[30] although the math is cumbersome. A second assumption can be made for short reaction times which will further simplify matters. Use of the remission function in eq 50 gives:

$$C_A = sC_o(k'_A - k'_P)^{-1}[f - f_P] \tag{51}$$

where f_P is the remission function of pure P. The time derivative of eq 51 is:

$$dC_A/dt = sC_o(k'_A - k'_P)^{-1}df/dt \tag{52}$$

Equations 51, 52, and 49 may be combined and rearranged for integration knowing that at $t = 0$, $f = f_A$, where f_A is the remission function of pure A to give:

$$\int_{f_A}^{f} \frac{df}{(1 + R)(f - f_P)} = -(k'_A/C_o)\phi I_o t \tag{53}$$

The value of R changes much slower with time than f ($0 \leq R \leq 1$, $\infty \geq f \geq 0$) so that $(1 + R)$ may be considered approximately constant and taken out of the integral sign. After integration the result is:

$$(1 + R)^{-1} \ln[(f - f_p)/(f_A - f_p)] \cong -(k'_A/C_o)\phi I_o t \qquad (54)$$

Thus a plot of the left hand side of the equation versus time should yield a straight line, and if C_o, k'_A and I_o are known, the values of the quantum yield may be determined. According to the Kubelka-Munk theory $k'_A = 2k_A$ where k_A is the true coefficient of absorption of A.[30] Although not critical to the present discussion the scattering coefficient s has been reported to be proportional to the inverse of the mean particle diameter.[44]

Particle model. In 1971, Simmons used a model similar to Melamed's[45] to describe the reflectance properties of weakly absorbing samples.[29] Simmons defined a parameter A to be the fraction of radiation absorbed by the particle, such that

$$A = \frac{(1 - \bar{m}_e)(1 - a)}{1 - \bar{m}_i a} \qquad (55)$$

where $\bar{m}_e$ and $\bar{m}_i$ stand for the average fraction of light reflected externally from a particle, and the average fraction of light which is internally reflected back into the particle, as previously stated. The coefficient, a, stands for the transmission of the particle according to Beers law

$$a = \exp(kL) \qquad (56)$$

Here k is the absorption coefficient and L is the average distance that the light which enters a particle travels before reaching the surface again.

Using arguments similar to Melamed, he then derived an equation for R:[29]

$$R = [1 - (2A - A^2)^{\frac{1}{2}}]/1 - A \tag{57}$$

It has been shown[29] that the average distance L across a sphere of diameter, d, is:

$$L = 2/3d \tag{58}$$

Equations 55, 56, and 58 can be combined to give

$$A = \frac{(1 - \bar{m}_e)[1 - \exp(-2kd/3)]}{1 - \bar{m}_i \exp(-2kd/3)} \tag{59}$$

In the case of weakly absorbing solids two simplifying assumptions may be made. Since A will be small, for a weak absorber, A^2 in eq 57 may be neglected and performing the division indicated will give:

$$R = 1 - (2A)^{\frac{1}{2}} + A - \ldots = \exp[-(2A)^{\frac{1}{2}}] \tag{60}$$

when the value of kd in eq 59 is small, a power series expansion of the exponential terms may be made with only the first two terms being retained as follows:

$$A = \frac{(1 - \bar{m}_e)2kd/3}{1 - \bar{m}_i + 2kd\bar{m}_i/3} = (1 - \bar{m}_e)(2kd/3)/(1 - \bar{m}_i) \tag{61}$$

if the term $2kd\bar{m}_i/3$ in the denominator is considered negligibly small. It can be shown[29] that:

$$\eta^2 = (1 - \bar{m}_e)/(1 - \bar{m}_i) \tag{62}$$

where η is the refractive index, the substitution of eq 62 into 61 gives:

$$A = \eta^2 2kd/3 \tag{63}$$

Finally eq 63 may be placed into eq 57 to give the reflectance:

$$R = \exp[-2\eta(kd/3)^{\frac{1}{2}}] \tag{64}$$

The derivation of the quantum yield then proceeds as follows. The rate of disappearance of reactant A from the ith particle below the surface has been shown[31] to be:

$$dC_i/dt = -\phi\epsilon\eta^2 C_i I_i (1 + R_i^2) \tag{65}$$

where ϵ is the molar extinction coefficient, η is the refractive index, C_i is the concentration of A in the ith particle, R_i is the reflectance and $I_i(1 + R^2)$, the intensity of the light incident on the ith particle.

The reflectance of the ith particle that contains both a reactant and a product which absorb is obtainable from eq 64 and is as follows:

$$R_i = \exp[-2\eta(d/3)^{\frac{1}{2}}(k\frac{C_i}{C_o} + k_P\frac{C_{Pi}}{C_o})^{\frac{1}{2}}] \tag{66}$$

where k_P is the absorption coefficient of the product and C_{Pi} is the concentration of product in the ith particle. By using the relationship

$$C_o = C_i + C_{Pi} \tag{67}$$

Equation 66 can be rearranged in terms of C_i to give:

$$C_i = C_o \frac{(\ln R_i)^2 - (\ln R_p)^2}{(\ln R_c)^2 - (\ln R_p)^2} \tag{68}$$

where R_c is the reflectance of pure reactant and R_p is the reflectance of pure product. The time derivative of eq 68 is:

$$\frac{dC_i}{dt} = C_o \frac{2\ln R_i}{(\ln R_i)^2 - (\ln R_c)^2} \frac{d\ln R_i}{dt} \tag{69}$$

Equations 68 and 69 may be substituted into eq 66 and rearranged for integration, making use of the fact that at t = 0, $R_i = R_c$ to give:

$$\int_{R_A}^{R_i} \frac{2\ln R_i d\ln R_i}{(1 - R_i^2)[(\ln R)^2 - (\ln R_p)^2]} = -\int_0^t \phi \epsilon n^2 I_i dt \tag{70}$$

Since only the reflectance at the surface can be measured the subscript (i) may be dropped to give:

$$\int_{R_c}^{R} \frac{2\ln R d\ln R}{(1 + R^2)[(\ln R)^2 - (\ln R_p)^2]} = -\phi \epsilon n^2 I_o t \tag{71}$$

A plot of the integral values versus time should give a straight line plot whose slope is $-\phi \epsilon n^2 I_o$, and if ϵ, n, and I_o are known, ϕ may be determined. This, however, is fairly complicated and can be simplified if the reaction time is small.

First the integral is integrated by parts:

$$\int_{R_A}^{R} \frac{2\ln R d\ln R}{(1+R^2)[(\ln R)^2-(\ln R_p)^2]} = \frac{1}{1+R^2} \ln\left[\frac{(\ln R)^2-(\ln R_p)^2}{(\ln R_c)^2-(\ln R_p)^2}\right]$$

$$+ \int_{R_A}^{R} \frac{2R^2}{(1+R^2)^2} \ln\left[\frac{(\ln R^2)-(\ln R_p)^2}{(\ln R_c)^2-(\ln R_p)^2}\right] d\ln R \qquad (72)$$

This can be rearranged, combining integrals to give:

$$\frac{1}{1+R^2} \ln\left[\frac{(\ln R)^2-(\ln R_p)^2}{(\ln R_c)^2-(\ln R_p)^2}\right] = \int_{R_A}^{R} \left[\frac{\ln R}{(\ln R)^2-(\ln R_p)^2} - \frac{R^2}{1+R^2}\right.$$

$$\left. \cdot \frac{(\ln R)^2-(\ln R_p)^2}{(\ln R_c)^2-(\ln R_p)^2}\right] \frac{2 d\ln R}{(1+R^2)} \qquad (73)$$

Finally, observing that for small extents of reaction for which $R_A \sim R$,

$$\left|\frac{\ln R}{(\ln R)^2-(\ln R_p)^2}\right| >> \left|\frac{R^2}{1+R^2} \ln\left[\frac{(\ln R)^2-(\ln R_p)^2}{(\ln R_c)^2-(\ln R_p)^2}\right]\right| \qquad (74)$$

eq 72 may be rewritten as follows:

$$\int_{R_A}^{R} \frac{2\ln R d\ln R}{(1+R^2)[(\ln R)^2-(\ln R_p)^2]} \cong \frac{1}{1+R^2} \ln \frac{(\ln R)^2-(\ln R_p)^2}{(\ln R_A)^2-(\ln R_p)^2} \qquad (75)$$

Thus for short reaction times where the extent of reaction is small:

$$\frac{1}{1+R^2} \ln \frac{(\ln R)^2-(\ln R_p)^2}{(\ln R_c)^2-(\ln R_p)^2} \cong -\phi\varepsilon\eta^2 I_o t \qquad (76)$$

A plot of the left hand side of eq 76 versus time, should yield a straight line whose slope is equal to $-\phi\varepsilon\eta^2 I_o$. Thus as in previous

treatments the quantum yield is determined from the slope of the line.

EXPERIMENTAL

Preparation of Reagents

Preparation of $[Rh(NH_3)_5Cl]Cl_2$. Rhodium trichloride $[RhCl_3 \cdot 1.8H_2O]$ was obtained from Engelhard and used without further purification. The chloride salt was converted to the chloropentaammine chloride complex[46] as follows. An aqueous solution (16 mL) containing the hydrated rhodium chloride (1.22 g) and ammonium chloride (1.53 g) was stirred and heated to 75 °C in a warm water bath. Ethanol (4 mL) was then added. After 3 min. of constant (magnetic) stirring, the reaction mixture was cooled to 35 °C. The addition of concentrated ammonium hydroxide solution (7 mL) to the dark brown solution precipitated the chloropentaammine chloride in the form of dull yellow crystals. After two min of additional stirring the solution temperature had risen to 40 °C. Subsequent to cooling in an ice/water bath, the filtered product was washed once with concentrated ammonium hydroxide (2 mL) and twice with small portions (2 mL) of ethanol. The air dried precipitate recovered, weighed 1.3 g. [Calc. 1.7 g].

Preparation of $[Rh(NH_3)_5I](ClO_4)_2$. According to Jorgensen[47] complexes of the type $(Rh(NH_3)_5X)Y_2$ ($X = Cl^-, Br^-, I^-$; $Y = Cl^-, Br^-, I^-, NO_3^-, SiF_6^-$) may be prepared with high yield and purity. The reaction sequence is similar in all cases so only the case where $X = I^-$ and $Y = ClO_4^-$ (a modification) will be considered. A mixture containing the chloropentaammine (1 g) prepared above, and water (40 mL) was heated to 90 °C in a hot water bath. Then a solution of 1.5 M sodium hydroxide (10 mL) was added.[48] The solution was stirred for 45 min at 90 °C. The mixture was then cooled to room temperature

and hydroiodic acid (47%, 45 ml) was added with stirring. A pale yellow precipitate, $[Rh(NH_3)_5OH_2]I_3$, formed. After cooling in an ice bath and filtering, the product was washed twice with hydroiodic acid (47%, 2 mL portions) and once with ethanol (2 mL). The crystalline product was mixed with 3 M hydroiodic acid and heated to 80° C for 1.75 h. This reaction was performed in a hood whose front glass panel had been covered previously with aluminum foil. This considerably reduced the amount of light reaching the photo-sensitive material formed. Illumination in this hood came from a red Kodak safelight during this reaction as well as the subsequent exchange reaction (see below). The crystals were cooled, filtered and washed as described above for the aquopentaammine complex. This precipitate $[Rh(NH_3)_5I]I_2$ was mixed with 6 M perchloric acid (40 mL) and stirred at room temperature for 45 min. During this time the solid crystalline phase was always present. The crystals were then filtered and washed twice with aliquots of concentrated perchloric acid (2 ml) and twice with ethanol. The air dried product $[Rh(NH_3)_5I](ClO_4)_2$ displayed absorption bands at 417 nm and 279 nm, which agreed with the literature values[49] of 416 nm and 278 nm.

It should be mentioned that although the preparation of $[Rh(NH_3)_5I](ClO_4)_2$, according to Bushnell[50], was used to prepare the starting material for the photoaquation reaction in solution,[17] this method has several problems. The reaction sequence has many steps and does not go cleanly for the most part. Thus, isolation of intermediates and purification of the product results in very low yields. For example, the Bushnell procedure requires the addition of

perchloric acid to precipitate $[Rh(NH_3)_5OH_2](ClO_4)_3$. The modification of Jorgensen presented here, using hydroiodic acid, allows for the immediate separation of the relatively insoluble triiodide analog. Addition of NaI and heat to a solution of the perchlorate yields a mixture of the triiodide and the desired product $[Rh(NH_3)_5I]I_2$, whereas, simple heating of a suspension[51] of the aquotriiodide in 3 molar hydroiodic acid yields essentially only $[Rh(NH_3)_5I]I_2$.[52] Initial dissolution of the diiodide was also found to be unnecessary. The outer sphere iodide ions exchanged readily with perchlorate (from perchloric acid) at room temperature. The weight percent yield when using Buchnell's method was usually between 10% and 50% while that obtained by Jorgensen's was nearly 100% of the starting pentaammine chloride. The purity of the compound, as evidenced by its visible ultraviolet spectrum varied between 13% and 90% for Bushnells' procedure while the purity of the material obtained by the Jorgensen method was in very good agreement with the literature[49] (greater than 95%). It should be mentioned that the 90% obtained using Bushnell's procedure included two recrystallizations while the 95% purity obtained via the preferred method was prior to recrystallization.

Thus, because of the problems of the Bushnell preparation which included 1) necessary separation of intermediates, 2) large volumes necessary for dissolution of the slightly soluble intermediates and overall low purity, this method should be avoided in favor of the one outlined in the procedure section which offers a high yield of a relatively pure product with very few isolation steps.

Preparation of $[Rh(NH_3)_5OH_2I](ClO_4)_2$. The iodoaquotetraammine was obtained by irradiating aqueous solutions of the iodopentaammine salt with room light and/or the light source used in the photolabilization experiments described below. The visible spectrum of the product corresponded with the literature.[16] This product was not isolated here.

Preparation of NaHY zeolite. To a rapidly stirring solution of acetic acid (4 L; 10^{-4} M) at room temperature was added 5 gm of NaY zeolite (Linde lot #3365-94). As the exchange proceeded the pH of the solution increased. After 12 hrs of stirring, more acetic acid (1 M) was added, drop by drop, from a burette, to return the solution to a pH of 4. An additional 12 hrs of stirring was not accompanied by a further change in pH, therefore the exchange was considered complete. The solution was filtered on a fine-scintered glass buchner funnel, washed 2 times with ca. 50 mL portions of distilled deionized water and dried by drawing air through the sample. The crystalline integrity of the zeolite was verified by comparing the X-ray powder pattern before and after hydronium ion exchange. The extent of exchange was deduced from the approximate amount of acetic acid needed to maintain the solution at pH 4. The applicable equation is:

$$[Na^+_{(exc)}] \simeq [Ac^-] = \frac{K_d[HAc]}{[H^+]} \qquad (77)$$

where $Na^+_{(exc)}$, Ac^- and HAc refer to the sodium ions, acetate ions and acetic acid in solution at equilibrium.

The extent of hydronium ion exchange was approximated using eq (39) and was found to be ca. 1.7×10^{-3} moles H_3O^+/g. It is

assumed that these ions were exchanged for sodium ions. For a typical sodium Y zeolite of composition:[53]

$$Na_{56}[(AlO_2)_{56}(SiO_2)_{136}]\cdot 250H_2O$$

This corresponds to the exchange of approximately 50% or roughly 28 sodium ions per unit cell.[54]

Preparation of $[Rh^{III}(NH_3)_5I]$/NaHY zeolite. Into 700 ml of an aqueous solution of iodopentaamminerhodium(III) perchlorate (0.112 g, 2.2×10^{-4} mole) was added 0.568 g of the previously prepared NaHY zeolite, with stirring at room temperature. A black-taped flask was used to prevent the photoreaction from occurring. After 24 h the zeolite was filtered and washed once with 50 mL of distilled deionized water, and dried as described above for NaHY. The pH of the solution was observed before and after the exchange and it was noted to decrease slightly. The filtrate was also observed to be colored yellow after the exchange was complete. The optical density was observed at 417 nm and the concentration of $[Rh(NH_3)_5I]^{2+}$ left in solution, [C], was calculated using Beers law:

$$[C] = A/\varepsilon\ell \qquad (78)$$

The symbols A and ε refer to the measured optical density and the extinction coefficient of iodopentaamminerhodium(III) in solution. The extent of exchange was determined by difference.

During the iodopentaamminerhodium(III) exchange, it was noticed that the pH of the aqueous phase decreased. This was probably due to the exchanging out of some of the hydronium ions then present. The

final pH of this solution was observed to be less than 4. X-ray powder patterns obtained before and after this exchange were compared to each other and to a powder pattern of the parent NaY. No loss in crystallinity resulted from the hydronium ion exchange; however, the powder pattern obtained after complex exchange showed increased, as well as decreased, peak intensities making an accurate estimate of crystallinity loss impossible. The amount of complexed rhodium exchanged in was taken as the difference betwen the moles determined from the amount of complex weighed out and that determined from the optical density of the filtrate after the exchange and was determined to be 2.6×10^{-4} moles/gm or ca. 2.7% rhodium by weight. At this exchange level, there was a five fold excess of hydronium ions even if the rhodium exchange was exclusively in favor of hydronium ion removal, therefore the rate could be considered independent of hydronium ion concentration.

Light Source and Calibration

Photolysis apparatus. A mercury vapor lamp from General Electric (100 W, H100 A4/T) was coupled with a collimating lens and chemical filter solutions to isolate the 435.8 nm line.[55] The lamp was enclosed in a housing which permitted light to travel in only one direction. The focal length of the lens (f) was found by using the formula:

$$\frac{1}{f} = \frac{1}{p} + \frac{1}{q} \qquad (79)$$

where p is the distance from the bulb to the lens and q is the distance from the lens to the point where the image of the bulb is focused.

The lens was then placed one focal length away from the bulb so that the rays of emerging light would be parallel.

The filter solutions were contained in two cells, each 10 cm in length. A common central Pyrex window separated the solutions. A water-cooled jacket surrounded both cells to prevent uneven heating of the cells due to infrared absorption by the solutions. The cell and the cooling jacket are depicted in Figure 1. The filter consisted of two solutions. The first was a solution of sodium nitrite in water (7.5 g/100 mL) and the second solution was an aqueous mixture of copper sulfate pentahydrate (0.44 g) and concentrated ammonium hydroxide (18 mL) diluted to 100 mL.

Ferrioxalate Actinometry. [56] The intensity of the light source was determined by using the wet chemical technique titled above. A modified version[56a] of the original preparation[56b] was adopted here since it eliminated the possiblity of shelf decomposition of the actinometer. Iron and oxalate solutions were prepared in separate vessels and were photochemically inert until they were mixed and diluted to give a fresh actinometer solution. The concentration of the iron solution was found by using the following method.[57] A known volume of the solution was reduced with hydroxylamine hydrochloride. After the addition of 1,10-phenanthroline and a volumetric dilution, the optical absorbance of this ferrous phenanthroline solution was measured at 510 nm where its extinction coefficient is 1.10×10^4 cm^{-1} M^{-1}. The concentration of this diluted solution was found using Beer's law (eq 78).

It should be noted that an error exists in the modification as

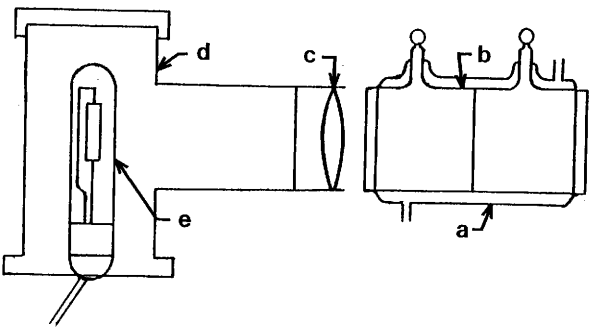

Figure 1. Exciting source: (a) cooling jacket for (b) solution filters; (c) lens; (d) lamp housing; (e) mercury vapor lamp.

reported by Murov.[56a] The third solution preparation reads "Ferrous sulfate solution" but it should read "Ferric sulfate solution." The rest of the procedure is straightforward and will not be discussed further. The light source intensity was calculated by using eq 13 arranged in the following form:

$$I_c = \frac{[P]}{\phi(1-10^{-\varepsilon[C]l})t} \tag{80}$$

The extinction coefficient, ε, is of ferrioxalate at 435 nm. The actual concentration of product formed was found using eq 78, where ε in this case stands for the molar absorptivity of ferrous phenanthroline at 510 nm. The intensity of the source was constant during each run, provided 30 min or more was allotted for the lamp to warm up. Since the light intensity was seen to vary from one run to the next, the light source was calibrated at the beginning of each run.

It was noticed that if the calibration cell was placed as much as 0.5 cm out of position the intensity change was less than 10% of the original intensity. In addition to slight changes in the intensity of the mercury vapor lamp (due to slight variations in lamp position), there was an overall decrease in the output of the lamp over the series of reactions. During each individual reaction, however, the light source intensity appeared to remain essentially constant (Table I). The source intensity was obtained at the beginning of each experiment.

The light used by the Beckman Acta III spectrophotometer to determine the concentration of reacted ferrioxalate also caused slight decomposition of the actinometer solution. This error was negligible

Table I. Light Source Intensity

Run	Conditions	I^a, einstein/cm^2 min	Total Time, min
1	Initial Trial	$4.3\pm0.3 \times 10^{-8}$ (4)	75
	Liquid		
2	6.69×10^{-3} M	$4.0\pm0.3 \times 10^{-8}$ (3)	70
3	5.35×10^{-3} M	$3.6\pm0.1 \times 10^{-8}$ (3)	65
4	6.42×10^{-3} M	$3.6\pm0.1 \times 10^{-8}$ (3)	60
	Solid		
5	37 μm	$3.2\pm0.1 \times 10^{-8}$ (b)	-
6	32 μm	$2.9\pm0.1 \times 10^{-8}$ (3)	57
7	40 μm	$2.8\pm0.1 \times 10^{-8}$ (3)	48
8	36 μm	$2.5\pm0.1 \times 10^{-8}$ (3)	60
9	38 μm	$2.1\pm0.1 \times 10^{-8}$ (3)	47
10	Reflectance[c]	$2.2\pm0.1 \times 10^{-7}$ (3)	12

a, Average value with number of determinations in parentheses. b, Not specifically measured, found by interpolation. c, unfiltered source intensity.

since 10 min of spectrometer radiation resulted in less than a 2% change in the absorbance value. Decomposition due to dark (thermal) reactions was slow; however, unused portions of the actinometer solution had to be discarded after two weeks due to the buildup of product.

Irradiation of $[Rh(NH_3)_5I](ClO_4)_2$ In Solution

All solutions were degassed by bubbling chromium-scrubbed[58] nitrogen through them before and during reaction. All irradiation experiments were conducted under darkroom conditions where the only illumination other than the exciting source came from one red and one amber Kodak safelight. Solutions of varying concentration and ionic strength were irradiated and the formation of product was followed by observing the change in pH. In a typical experiment a solution of iodopentaamminerhodium(III) perchlorate (6.3×10^{-3} M; final conc.) was adjusted to a pH of 3 (using $HClO_4$) and an ionic strength of 0.1 (using $NaClO_4$). An aliquot of this solution (3 ml) was placed in a quartz cell. The quartz cell had been covered beforehand with aluminum foil, except for the lower one square centimeter, on its front and back side so that the results obtained would be more easily comparable with those of the solid state reaction (cf. below). The filled cell was then placed in the IR-9 spectrophotometer in a position which was similar to that which was occupied by the solid sample in subsequent experiments (see below). A combination pH electrode was then immersed into the solution along with a micropipette (which functioned as the nitrogen bubbler).

The hydronium ion concentration $[H^+]$ in the soluton was found by the following equation:

$$pH = -\log([H^+] \cdot f_{H^+}) \tag{81}$$

where f_{H^+} is the activity coefficient of hydronium ion. The activity coefficient is related to the ionic strength (μ) of the solution by:

$$\log f_{H^+} = \frac{0.5\mu^{\frac{1}{2}}}{1 + 3\mu^{\frac{1}{2}}} \tag{82}$$

The ionic strength was determined in the usual way by the formula:

$$\mu = \tfrac{1}{2} \sum_i C_i Z_i^2 \tag{83}$$

where C_i is the concentration of the i^{th} ion and Z_i is the charge of that ion. The moles of hydronium ion consumed is equal to the number of complexes which reacted, thus the rate can be expressed by $\Delta P/\Delta t$. The quantum yield was obtained using eq 13, where I_o is measured in einsteins $\cdot$ cm^{-3} and the extinction coefficient at 435 nm was determined from the experimental absorbance.

Irradiation of $[Rh(NH_3)_5I]^{2+}$ Exchanged In NaHY

It should be remembered that prior to irradiation, all procedures involving the reactant were carried out under darkroom conditions. The exchanged zeolite was pressed into wafers which were $\leq$ 5 mg/cm^2, "thick." Since the wafers were very thin, these units were convenient. Each wafer was pressed to 500 kg$\cdot$$cm^{-2}$ for ca. 30 sec using a high-carbon steel dye. Then the wafer was cut into a rectangle (approximately 1 cm x 2 cm) for mounting into the sample holder. The sample holder was then lowered into the infrared cell described in Figure 2. The infrared cell was mounted on a bracket which was bolted

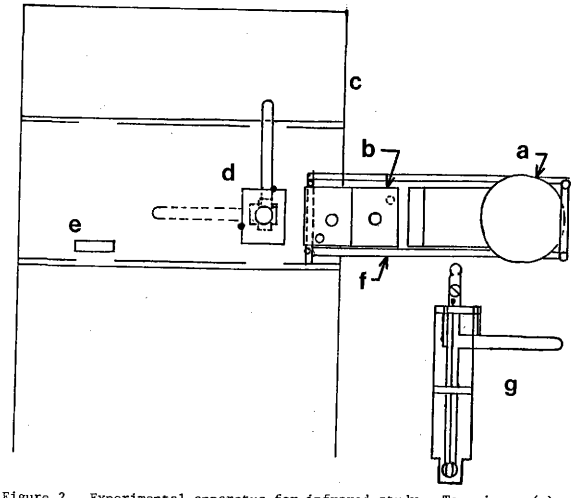

Figure 2. Experimental apparatus for infrared study. Top view: (a) light source; (b) filters cell; (c) Beckman IR-9 spectrophotometer; (d) infrared cell in position for irradiation, dotted lines represent position for infrared spectrum recording; (e) reference attenuator; (f) source/cell support; (g) side view of infrared cell and bracket.

to the infrared instrument. This permitted all the wafers to be oriented in a similar way with respect to the infrared beam. With the aid of two stops at 90° angles, a reproducible orientation of the cell with respect to the exciting visible source (described above), was also achieved. A typical experiment consisted of placing a precut wafer into the cell and placing the cell in the IR beam. After the glower current was set at 0.60 Amp, the slit mode was set to select, and the slit width was adjusted to 0.98 nm at 1350 cm^{-1} to give a resolution of cm^{-1}. Then in the transmission mode and on single beam, the gain was adjusted to give a 55% deflection of the pen at 1850 cm^{-1} where there was a window in all the zeolite spectra considered here. Typical gain settings were between 2% and 5%. The reference beam was then attenuated in the double beam mode to 75% deflection of the pen at 1850 cm^{-1}. Preliminary studies showed that a period of 8 and a scan speed of 80 cm^{-1}/min. give the best signal to noise response, thus these settings were used exclusively.

The IR transmission spectrum of the wafer was then recorded between 1200 cm^{-1} and 2000 cm^{-1}. Next the spectrometer was switched to the absorbance mode and the absorbance spectrum from 0 to 1 was recorded between 1250 and 1650 cm^{-1}. A 90° turn then oriented the wafer perpendicular to the visible source as described in Figure 2 (p.38) and the wafer was irradiated for a preset time interval. At the end of this time the cell was returned to its original position by a 90° turn in the opposite direction and the IR spectrum was again recorded. The buildup of ammonium ion at 1455 cm^{-1},[59] along with the decrease in the coordinated ammonia band at 1335 cm^{-1},[60] was followed for periods of between 210 and 240 min total accumulated irradiation

time. The moles of ammonium ion product per square centimeter was found from the infrared absorbance after the instrument was calibrated (see below). The quantum yield was then obtained using the various treatments described in the theory section.

Calibration of the IR-9 Spectrophotometer

The absolute amount of ammonium ion in the zeolite obtained from infrared absorption measurements resulted from the following calibration. Three solutions were prepared containing ~0.36 g, ~0.22 g, and ~0.50 g of ammonium chloride per liter. Approximately one gram of NaHY was added to each solution while stirring, and then they were heated to 50°-60 °C. A watch-glass cover over each prevented excessive solvent loss due to evaporation. After 24 h each of the solutions was allowed to cool. The exchanged zeolites were filtered and dried as described previously. Wafers of varying thickness were prepared for each concentration. The transmission spectrum of each wafer was recorded between 1200 cm^{-1} and 2000 cm^{-1} and its absorption spectrum was recorded between 1250 cm^{-1} and 1650 cm^{-1}. The absorbance of ammonium ion was found by drawing a smooth curve, as given by the initial spectra, to connect the two minima (Figure 3). This peak was then cut out and weighed. A graph of thickness (mg/cm^2) versus the weight of the peak was prepared for each extent of exchange. The total amount of ammonium ion in each of the three exchanged zeolites was found via a Kjeldahl determination for ammonium ion (see Appendix B). A plot of the concentration (moles/mg) of unitized thickness (mg/cm^2) of these standards versus relative peak area completed the calibration.

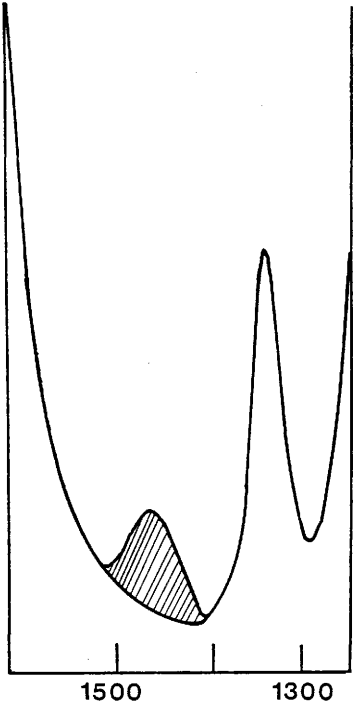

Figure 3. Infrared spectrum of the ammonium ion band at 1450 cm^{-1} and the zeolite background (lower portion). Relative peak areas were obtained from the weight represented by the shaded area.

As expected from Beers law, there was a linear correlation between the absorbance (measured as the weight of the paper under the peak) and the thickness of the wafer. A plot of the concentration of various HY samples with different loadings of ammonium ion versus the relative peak area for wafers of the same thickness showed a negative deviation from Beer's law at higher concentrations. For the photoaquation reaction under consideration, the maximum concentration of ammonium ion obtainable assuming 100% conversion was within the linear portion of the graph. Since the mathematical treatments applied to this system are reported in moles per square centimeter, the calibration graph constructed was that given in Figure 4.

Partial Dehydration and Irradiation of $[Rh(NH_3)_5I]Y$ Zeolite

The amount of water lost from a sample of the exchanged zeolite was determined using a McBain scale.[61] During a 12 h evacuation the sample was degassed to a final dynamic vacuum of 2.5×10^{-5} torr.

A second sample of the same exchanged zeolite was pressed and inserted into the IR-9 spectrophotometer as described previously. The infrared cell was then connected to the same vacuum line as was the McBain scale above. An infrared spectrum of this sample was obtained before the subsequent 12 h evacuation. A second infrared spectrum was taken before any visible irradiation of the sample occurred. This was followed by the visible irradiation procedure described above. Analysis of products was similar to that of the hydrated zeolite reaction.

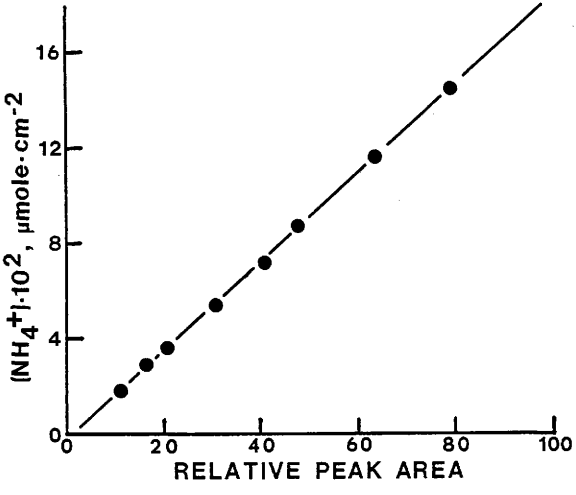

Figure 4. Calibration graph of ammonium ion concentration versus infrared absorption.

Reflectance Study

The light intensity of the reflectance source of the Cary 14 reflectance spectrometer was calibrated using ferrioxalate actinometry (see above).

A relatively thick pressed waver of exchanged Y zeolite was placed onto the sample side of the instrument with MgO as the reference. Initially the visible spectra was obtained from 380 nm to 650 nm. All subsequent runs went from 340 nm to 700 nm. The light source was turned on at the start of each run and off at the end. Recording of the spectrum began as soon as the recorder pen stabilized. In each case this occurred within 5 sec after the source was turned on. The decrease of the reactant, at 430 nm, and the increase of product, at 485 nm, were followed with respect to time.

In both reflectance studies the term on the left hand side of eq 54 or eq 76 was plotted as a function of time and the slope was related to the quantum yield.

Absolute Thickness

The absolute thickness of the wafers was determined using a goniometer. Small sections of the original wafers were mounted on a goniometer head and aligned so they were oriented edge on with respect to the lens. An internal, movable scale yielded the thickness to a precision of 4×10^{-3} mm.

A reasonably good correlation was found between the "thickness" as it is often reported for very thin wafers, in $mg \cdot cm^{-2}$, and the actual thickness measured in microns (10^{-6} m) as shown in Figure 5.

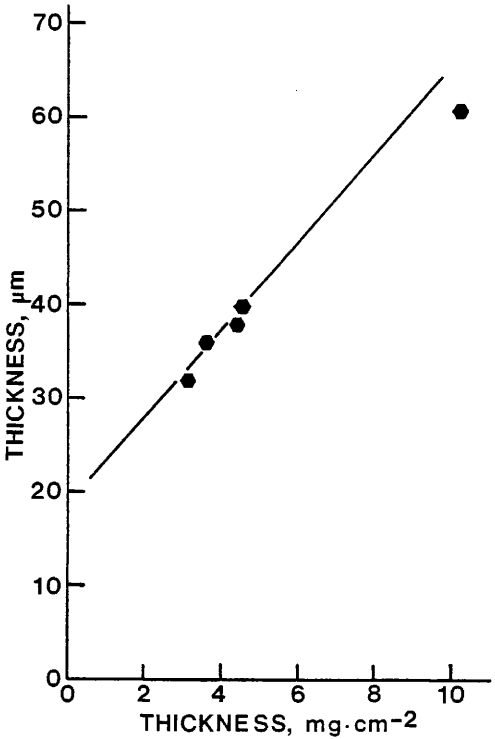

Figure 5. Correlation of the actual thickness of wafers of zeolite versus the empirical "thickness" measured in $mg \cdot cm^{-2}$. The wafers between 3 and 5 $mg \cdot cm^{-2}$ were formed under a higher pressure than the one at 10.2 $mg \cdot cm^{-2}$, thus this point was excluded from the linear least squares analysis.

This correlation is only strictly true for samples which were formed under the same pressure.

RESULTS

Quantum Yield in Solution

A plot of ammonia formation versus time for solutions of varying concentration and ionic strength, μ, shows the effects of these variables on the reaction rate (Figure 6). The rate of reaction ($\Delta P/\Delta T$) is seen to increase with increasing ionic strength as does the quantum yield. The pseudo-zero order approximation for small extents of conversion appears to be valid for the two larger concentrations, 6.6×10^{-3} M (a) and 6.4×10^{-3} M (c), as evidenced by the linear dependence of product formation with respect to time. The slight curvature present in the smaller concentration, 5.3×10^{-3} M (b), is probably due to the relatively low concentration. The quantum yield values obtained in this analysis are given in Table II.

The quantum yield for $[Rh(NH_3)_5I]^{2+}$ photoaquation was previously reported[17] to be 0.87±0.07 in solutions adjusted to 0.1 μ. In the present work a value of 1.06±0.08 was observed. These values are close to each other, especially when the limits of error are considered. The quantum yield determined in this work will be used for comparison unless specifically stated otherwise.

Determination of Quantum Yield in the Solid Phase by Infrared Spectroscopy

As the photoaquation of exchanged $[Rh(NH_3)_5I]^{2+}$ proceeded, the absorption band due to ammonium ion at ca. 1450 cm^{-1} increased as shown in Figure 7. Since the wafers could not be pressed in total darkness, a correction was made for the small amount of product

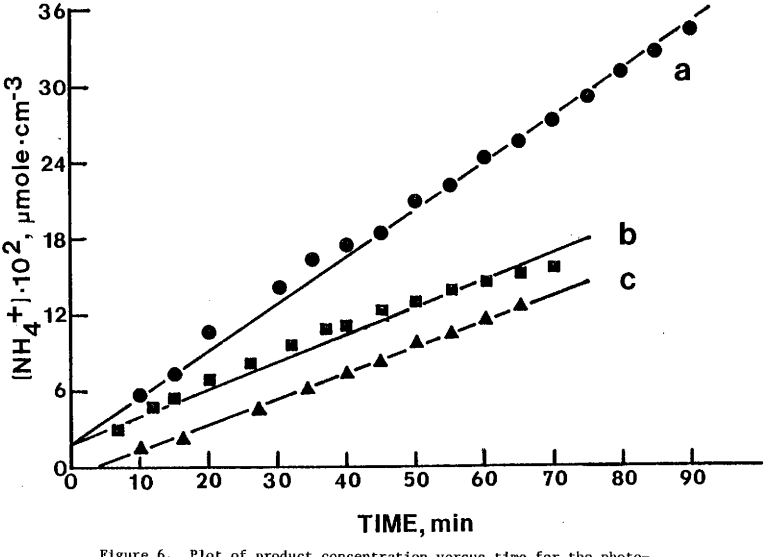

Figure 6. Plot of product concentration versus time for the photoaquation of $[Rh(NH_3)_5I]^{2+}$ in solution at 435 nm: (a) 6.42 x 10^{-3} M, 0.10μ; (b) 5.35 x 10^{-3} M, 0.08μ; (c) 6.69 x 10^{-3} M, 0.02μ.

Table II. Quantum Yield Values for the Photoaquation of $[Rh(NH_3)_5I](ClO_4)_2$ in Solutions of Varying Ionic Strength

Concentration	Ionic Strength	ϕ
6.69×10^{-3} M	0.020	0.52
5.35×10^{-3} M	0.083	0.65
6.42×10^{-3} M	0.10	1.06

Figure 7. Infrared spectra of the absorption due to ammonium ions at 1450 cm^{-1} after various periods of irradiation: (a) t= 0; (b) t=50 min; (c) t=240 min; (d) t=∞.

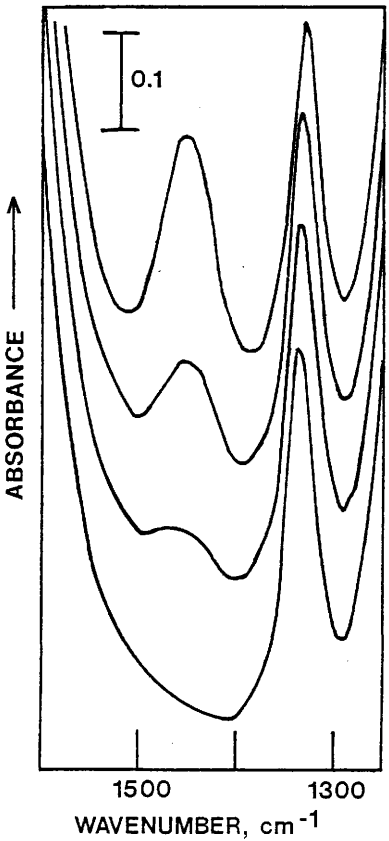
0.1
ABSORBANCE
1500
1300
WAVENUMBER, cm -1

(curve a) which appeared in the infrared spectrum before the start of the irradiation. This correction usually amounted to less than 2% of the moles of reactant initially present.

Pseudo-zero order approximation. Regardless of wafer thickness, a plot of product concentration versus time (Figures 8 and 9). straight line for relatively short reaction times, on the order of 50 min. After this time the rate is seen to fall off, possibly due to the decrease in reactant or to the buildup of a surface layer of product.

For short reaction times (≤50 min.) the quantum yield may be approximated by using eq 16. The fraction of light absorbed (1-R) was assumed to be constant during this time and was approximated to be 0.50 at 430 nm, which was the observed reflectance of a thick wafer containing the same loading of rhodium complex. The slope of the line (m) was equal to $\phi(1-R)I_o$, and since the intensity of the source (I_o) had already been measured, the quantum yield was found using:

$$\phi = \frac{m}{(1-R)I_o} \tag{84}$$

The actual value of the quantum yield obtained by this method is 0.22±0.02. The estimated error is mainly due to the assumptions that the reflectance is a constant and that the wafers are infinitely thick.

First order approximation. If it is assumed that the reactant concentration is important in determining the rate, which is reasonable considering initial concentrations on the order of 1×10^{-6} moles·cm^{-2}, then the rate should be expressed by a first order relationship. This

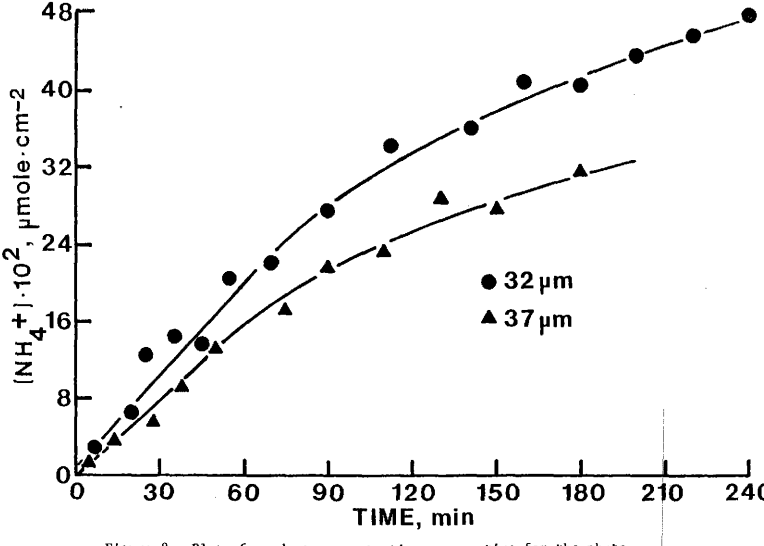

Figure 8. Plot of product concentration versus time for the photoaquation of $[Rh(NH_3)_5I]^{2+}$ in hydrated zeolite wafers.

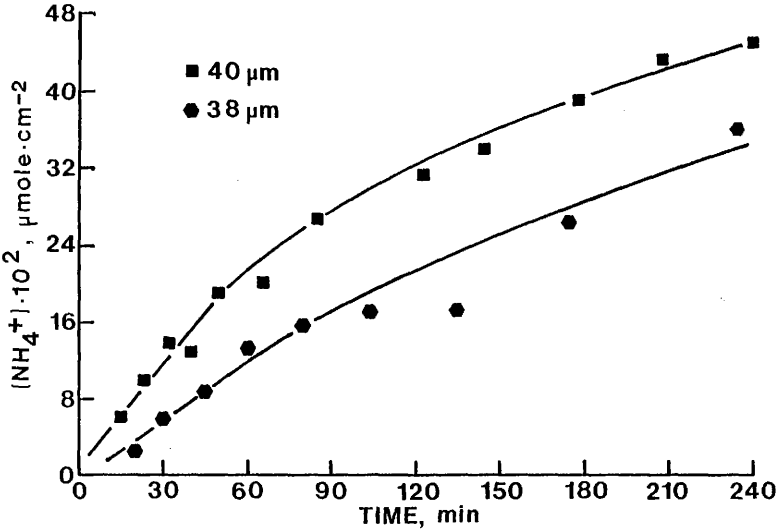

Figure 9. Plot of product concentration versus time for the photoaquation of $[Rh(NH_3)_5I]^{2+}$ exchanged in: ■ a hydrated zeolite; ● a partially dehydrated zeolite.

is shown graphically in Figure 10 and 11. The straight line obtained over the first 90 min confirms the applicability of this treatment.

Rearrangement of the integrated form of eq 38 yields the relationship between the slope of the line and the quantum yield:

$$\frac{\ln(C/Co)}{t} = -\phi n^2 \varepsilon I_o \qquad (85)$$

The extinction coefficient is assumed to be similar to that in solution; however, since concentrations are measured in moles/cm^2, the units of ε must be adjusted accordingly. For example:

$$270\ M^{-1}\ cm^{-1} = 270 \cdot \frac{1000\ cm^3}{m \cdot cm} = 270{,}000\ \frac{cm^2}{m} \qquad (86)$$

The value of the refractive index (n), although not specifically measured here is taken to be 1.50 which is within the range of the refractive indices of some naturally occurring zeolites.[62] Following this avenue led to a resultant quantum yield of 0.19±0.02.

Approximation due to the inner filter effect. The observed fall-off in reaction rate may have been due to build up of product at the surface. This behavior is represented by eq 42:

$$P = \frac{1}{k'} \ln(1 + \phi k' I_o t) \qquad (42)$$

The value of the quantum yield, ϕ, and attenuation constant, k', were approximated using a Taylor series expansion in terms of ($I_o t$) as follows:

$$P = \phi(I_o t) - \frac{\phi^2 k}{2}(I_o t)^2 + \frac{\phi^3 k^2}{3}(I_o t)^3 - \ldots \qquad (87)$$

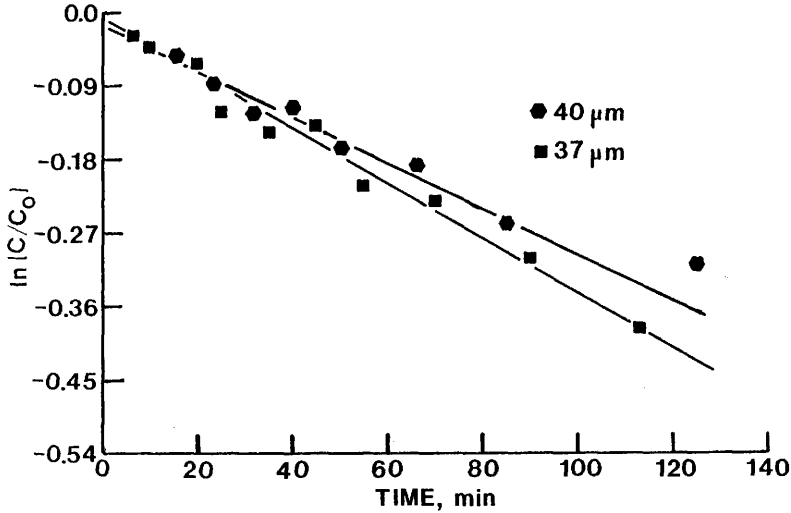

Figure 10. First order rate plot for the photoaquation of $[Rh(NH_3)_5I]^{2+}$ in hydrated zeolite wafers.

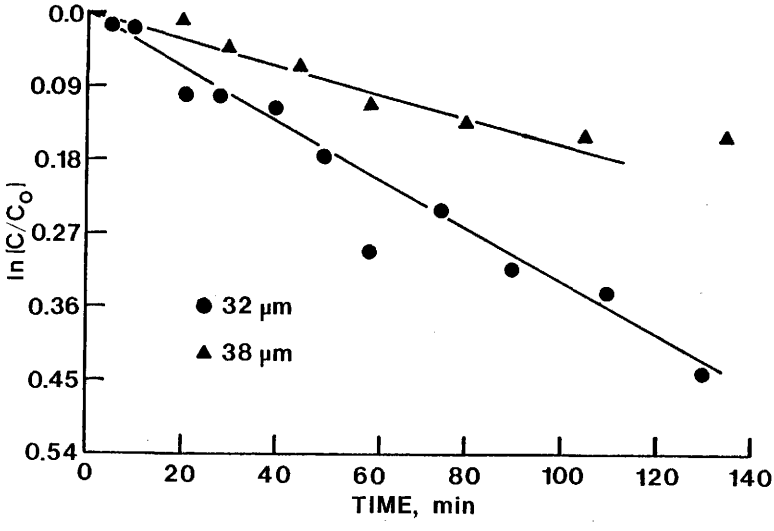

Figure 11. First order rate plot for the photoaquation of $[Rh(NH_3)_5I]^{2+}$ in: ● a hydrated zeolite; ▲ a partially dehydrated zeolite.

After assuming that the values of $(I_o t)$ were small, the series was truncated at the third term.

The coefficients of this equation were found using a non-linear least squares method and using matrix math to solve a set of linear equations.[63] For the generalized equation:

$$y = a_o + a_1 + a_2 x^2 + a_3 x^3 + \ldots \tag{88}$$

where a series of (x,y) points are known, the coefficients a_j may be found by setting up a matrix such that:

$$\begin{matrix} n & \Sigma x_i & \Sigma x_i^2 & \cdots & \Sigma x_i^m \\ \Sigma x_i & \Sigma x_i^2 & & & \\ \Sigma x_i^2 & & & & \\ \Sigma x_i^m & \Sigma x_i^{m+1} & & \cdots & \Sigma x_i^{2m} \end{matrix} \begin{matrix} a_o \\ a_1 \\ a_2 \\ \vdots \\ a_m \end{matrix} = \begin{matrix} \Sigma y_i \\ \Sigma x_i y_i \\ \Sigma x_i^2 y_i \\ \vdots \\ \Sigma x_i^m y_i \end{matrix} \tag{89}$$

where n is the number of points and m is the degree of the polynomial.

A programmable T.I. 59 calculator was used to sum all the x, x^2, y, xy, etc. values as described above. These values were then entered into a matrix subroutine of the calculator and the coefficients were obtained. These coefficients were then plugged into the Taylor series form of the original equation and a smoothed line was calculated by entering experimental exposure $(I_o t)$ values and calculating the theoretical amount of product.

The coefficients of the squared and cubed terms were first solved in terms of k', then they were set equal to each other to solve for the value of quantum yield. Twice this value was added to the value of the quantum yield obtained from the coefficient of the first term and the sum was divided by three so the coefficients would carry equal weight. This analysis led to a quantum yield value of 0.32 ± 0.04.

The experimental points and calculated fits for the various thickness and conditions are graphically displayed in Figures 12 and 13 A plot of ammonium ion concentration calculated by eq 84 versus the experimental concentration containing the data from all 3 hydrated wafers of different thicknesses are shown in Figure 14. If the solution to the equation were exact, the line obtained by this treatment should have a slope and correlation coefficient of one and an intercept equal to zero. The actual results are given in Table III.

There is one unfortunate deficiency in this method. The quantum yield may be obtained from the first non-zero coefficient:

$$\phi = a_1 \tag{90}$$

or by solving simultaneously the second and third coefficients for ϕ to give:

$$\phi = 4a_2^2/3a_3 \tag{91}$$

However, these two equations do not give exactly the same value for the quantum yield. Since the coefficients should be equally important, the quantum yield reported for each thickness gives equal weight to each of the coefficients as described earlier.

Figure 12. Effect of the inner filter on the photoaquation of $[Rh(NH_3)_5I]^{2+}$ in hydrated zeolite wafers: ▲, ■ represent experimental data points; ◆ represents the calculated concentration as determined from the truncated taylor series (see text). Where the calculated point overlaps the actual data, only the data point is shown.

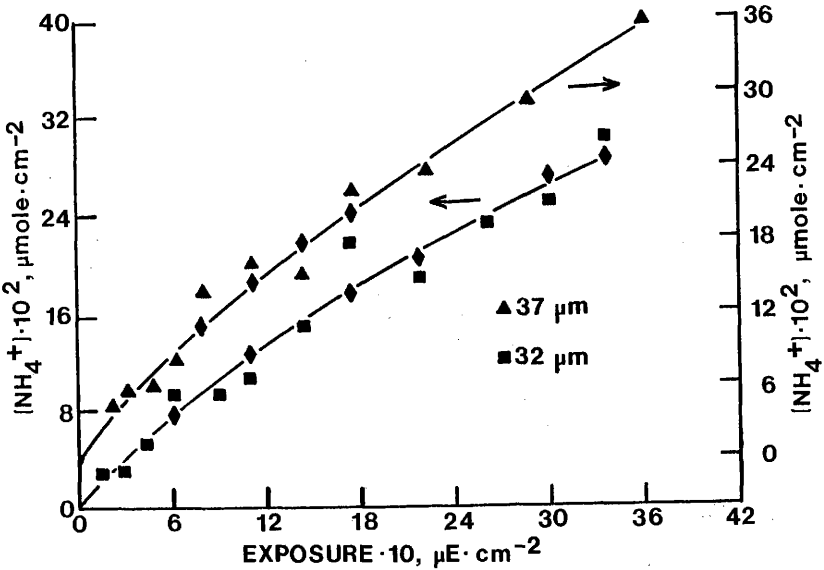
40
32
24
16
8
0
0
6
12
18
24
30
36
42
36
30
24
18
12
6
0
$[NH_4^+]\cdot 10^2$, µmole·cm^{-2}
$[NH_4^+]\cdot 10^2$, µmole·cm^{-2}
EXPOSURE·10, µE·cm^{-2}
▲37 µm
■32 µm

Figure 13. Effect of the inner filter on the photoaquation of $[Rh(NH_3)_5I]^{2+}$ in: ● the hydrated zeolite; ● the partially dehydrated zeolite; ◆ represents the calculated concentration as determined from the truncated Taylor series (see text). Where the calculated point overlaps the actual data, only the data point is shown.

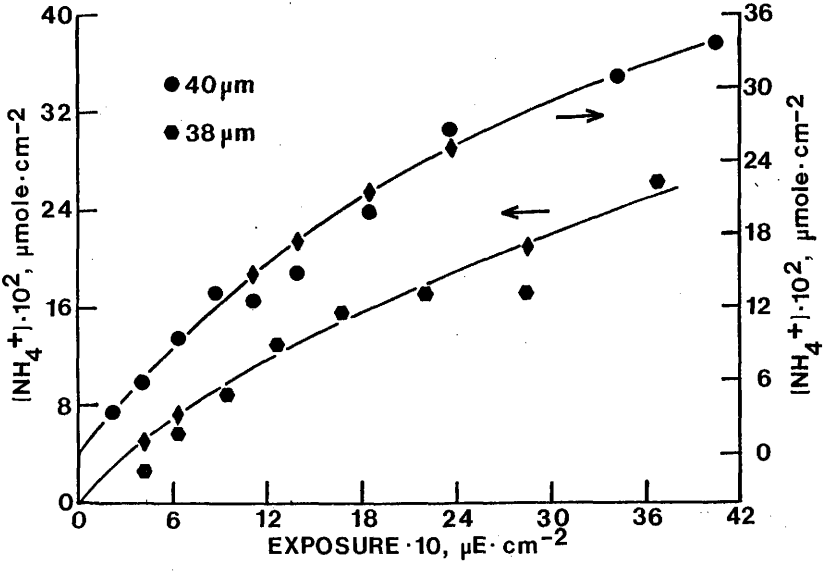
40
32
24
16
8
0
36
30
24
18
12
6
0
0
6
12
18
24
30
36
42
● 40 μm
● 38 μm
[NH4+]·10-2, μmole·cm-2
[NH4+]·10-2, μmole·cm-2
EXPOSURE·10, μE·cm-2

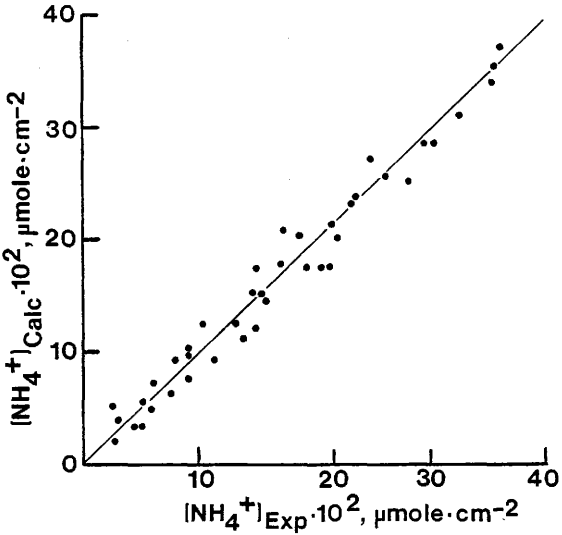

Figure 14. Correlation of the experimental product concentration versus that obtained by the non-linear least squares analysis.

Table III. Correlation Between Calculated Product Concentration and Experimental Data

Thickness	Slope	Intercept	r
32 μm	0.957	-1.34×10^{-8}	0.997
37 μm	1.016	-3.41×10^{-9}	0.988
40 μm	0.999	1.40×10^{-9}	0.995
38 μm[a]	0.948	4.16×10^{-8}	0.969

All wafers were hydrated except a, which was dehydrated as described in the text. The symbol r stands for the correlation coefficient.

Effect of dehydration. Since evacuation at ca. 100° C was accompanied by severe reactant decomposition (in the absence of light) recourse was made to a 12 h evacuation at room temperature. Even at these relatively mild conditions, water loss was accompanied by partial decomposition of the reactant, which amounted to approximately 12% of the initial reactant concentration. Before the start of the photoreaction 9.5% by weight of water, representing approximately 35% of the water available,[54] was removed. This decreased the number of available water molecules from about 50/complex to 35/complex.

The quantum yield might therefore be expected to remain relatively constant or decrease slightly. In fact the quantum yield appears to be about 70% of its original value according to the first order approximation. Conversely, the treatment which accounted for the surface layer of product shows that the value of the quantum yield has remained essentially constant.

Determination of Quantum Yield in the Solid Phase by Reflectance Spectroscopy

This method required only reflectance data to determine the quantum yield of the system so it provided an essentially independent way to verify the results obtained from the infrared study.

The decrease in reactant absorption at ~430 nm and the simultaneous increase in product absorption at 485 nm is shown very clearly in Figure 15. Note the appearance of isosbestic points at ~375 nm and 450 nm. This is evidence that there is probably only one reactant and one product.[64] The sample was removed and subjected to more intense radiation to drive the reaction to completion. Improper

Figure 15. Reflectance spectra showing the conversion of $[Rh(NH_3)_5I]^{2+}$, (430 nm) to $[Rh(NH_3)_5OH_2I]^{2+}$, (485 nm); scan rate 60 nm/min. Time at 430 nm: —— 1.5 min (t=0); ····· 6.67 min; ----13 min; — — 19.33 min; — · · — 37.5 min.

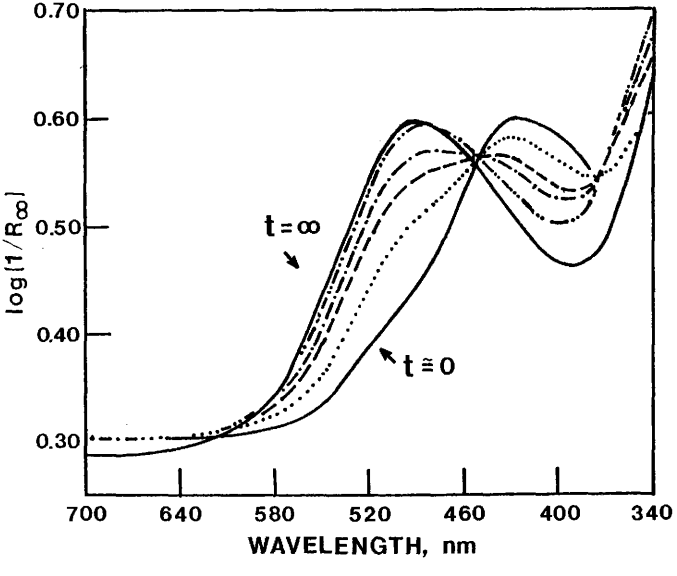
0.70
0.60
0.50
0.40
0.30
log(1/R∞)
t = ∞
t ≅ 0
700
640
580
520
460
400
340
WAVELENGTH, nm

replacement of the wafer resulted in a final spectrum (for t_∞) which does not cross the isosbestic point at 375 nm.

Since the compound began to react as soon as the spectrum was recorded, the initial reflectance at time zero was found by extrapolation (see Figure 16). It is interesting to note that there is a bathochromic shift in the reactive absorption band for the exchange complex, 430 nm, compared with this band in solution, 416 nm.

Continuous medium model. The rate of reaction was described by eq 54. The remission function (f) is assumed to vary much more rapidly than the reflectance (R) so R is considered a constant. A graph of $\frac{1}{1+R} \ln(\frac{f-f_\infty}{f_c-f_\infty})$ versus t yields a straight line (Figure 17), with a slope which is equal to $-2\varepsilon\phi I_o$. The extinction coefficient, ε, from solution data is 270,000 cm^2/mole. The unfiltered source intensity was determined to be 2.2 x 10^{-7} $E \cdot cm^{-2} \cdot min^{-1}$. Using these numbers and the observed slope of -0.0352, the quantum yield was calculated to be 0.30±0.02.

Particle model. The equation presented above is valid for weak absorbers where the product of the absorption coefficient and the particle diameter is small. If in addition to these two constraints the extent of conversion is also small, the following previously derived equation can be written:

$$\frac{1}{1+R^2} \ln \left(\frac{(\ln R)^2-(\ln R_p)^2}{(\ln R_c)^2-(\ln R_p)^2}\right) \cong \phi\varepsilon\eta^2 I_o t \qquad (76)$$

Actually this equation has been shown to be valid as described earlier when:

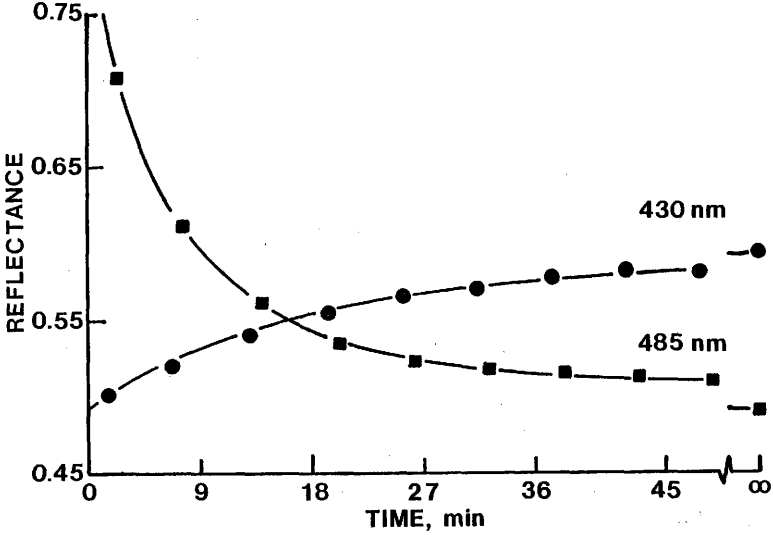

Figure 16. Variation of reflectance at: ● 430 nm and ■ 485 nm, during the photoaquation reaction. (The zeolite reflectance was taken as 1.0 at 700 nm.

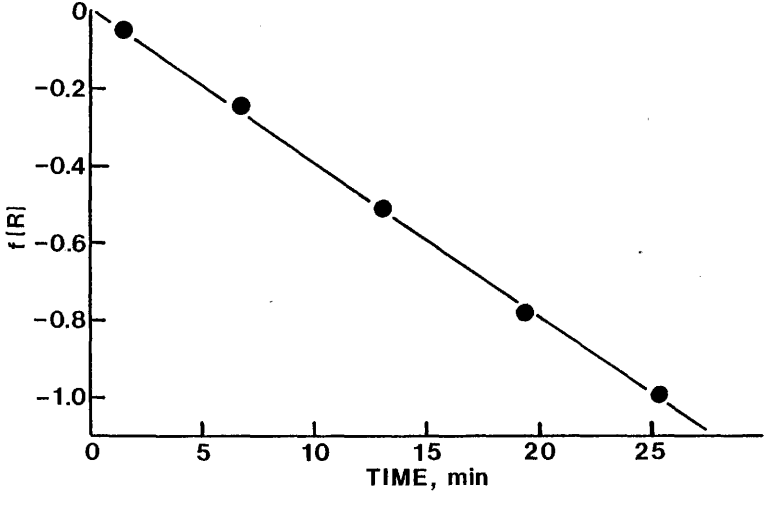

Figure 17. Application of the Kubelka-Monk theory to the rate of reaction. Plot of: $\frac{1}{1+R} \ln \frac{(f_\infty - f_p)}{(f_c - f_p)} = f(R)$ versus time (see eq 54).

$$\frac{\ln R}{(\ln R)^2-(\ln R_p)^2} >> \frac{R^2}{1+R^2} \ln \left[\frac{(\ln R)^2-(\ln R_p)^2}{(\ln R_c)^2-(\ln R_p)^2} \right] \qquad (92)$$

Table IV shows the results of this comparison for the reaction in question, as well as the percent difference for the reflectance data collected at 430 nm where $R_A = 0.495$ and $R_p = 0.594$, (Figure 16, p 70). One should observe that the percent difference in every case is less than 6 percent which is well within the range considered acceptable for this treatment.[32] The rate plot illustrating eq 76 yields a fairly straight line (Figure 18). The slope of this line is -0.0415 min^{-1} which results in a quantum yield of 0.32±0.02. The error in this case is approximated from the percent difference as given in Table IV.

Table IV. Validity of eq 74 Over the Experimental Reflectance Range

$$\underbrace{\frac{\ln R}{(\ln R)^2 - (\ln R_p)^2}}_{\text{I}} \gg \underbrace{\frac{R^2}{1+R} \ln \frac{(\ln R)^2 - (\ln R_p)^2}{(\ln R_c)^2 - (\ln R_p)^2}}_{\text{II}}$$

R	I	II	(II/I)·100%
0.501	-3.349	-0.031	0.093
0.520	-4.184	-0.146	3.48
0.541	-5.790	-0.311	5.37
0.555	-7.813	-0.461	5.90
0.564	-10.105	-0.586	5.80
0.571	-13.124	-0.712	5.42
0.578	-18.779	-0.881	4.69

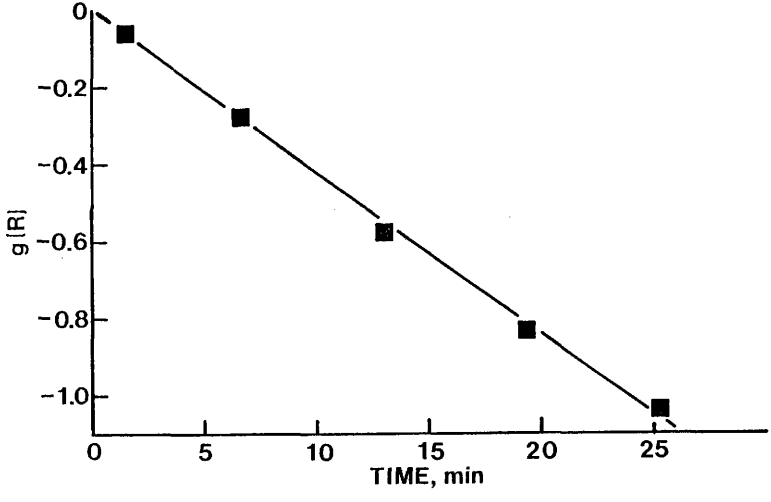

Figure 18. Application of particle model theory to the rate of reaction.

Plot of: $\frac{1}{1+R^2} \ln \frac{(\ln R)^2 - (\ln R_p)^2}{(\ln R_c)^2 - (\ln R_p)^2} = g(R)$ versus time (see eq 76)

DISCUSSION

The quantum yield values obtained for various thicknesses and experimental conditions from the various methods of approximation employed are summarized in Table V. Both the pseudo-zero and first-order approximations lead to a relatively low quantum yield, presumably because absorption by the product was not considered. It was assuring to note that the quantum yield obtained by infrared, in which product absorption is accounted for, is the same as the quantum yield obtained by reflectance spectroscopy, 0.30±0.02. Thus, it is shown that the quantum yield for the photoaquation of $[Rh(NH_3)_5I]^{2+}$ in the zeolite is approximately 30% of that obtained in solution, where ϕ = 1.06±0.07.

Wafers as thick as 40 μm exhibited some discoloration on the backside of the wafer due to the formation of product. The reaction followed by infrared were observed for the first 38-47 mole % conversion. After this time the reaction was driven to completion using multiple sources which were directed toward both sides of the wafer. These sources consisted of unfiltered ultraviolet and visible light. After 12 hours of additional radiation the mole % conversion increased to 95-98%. An accurate extent of conversion for the reflectance sample was impossible to measure since a similar radiation treatment resulted in no discoloration on the back side of the infinitely thick (61 μm) wafer and infrared scattering prohibited an accurate measurement of its absorption spectrum.

Table V. Quantum Yields from the Photoaquation of $[Rh(NH_3)_5I]^{2+}$ in Zeolite Y.

Thickness μm (mg/cm^2)	Environment[a]	ϕ	$\overline{\phi}$[b]
	A) Pseudo zero Order		
32 (3.1)	Air	0.20	
37[c] (4.1)	Air	0.22	0.22±0.02
40 (4.5)	Air	0.25	
38 (4.4)	Vac	0.17	
	B) First Order		
32 (3.1)	Air	0.20	
37[c] (4.1)	Air	0.19	0.19±0.01
40 (4.5)	Air	0.18	
38 (4.4)	Vac	0.13	
	C) Surface Attenuation		
32 (3.1)	Air	0.28	
37[c] (4.1)	Air	0.32	0.32±0.04
40 (4.5)	Air	0.36	
38 (4.4)	Vac	0.29	
	D) Reflectance		
61 (10.2)	Air[d]	0.30	
61 (10.2)	Air[e]	0.32	

a, All the spectra run at room temperature, wafers were reacted in the presence of air or in vacuo(P= 1 x 10^{-5} torr) b, Average value for the various hydrated wafers. c, Obtained from interpolation (Figure XV). d, Using eq 54. e, Using eq 76.

Although the observed apparent quantum yield, ~0.30, in the solid is much less than that observed in solution, ~1.0, this value is by no means disappointingly small. On the contrary, considering the constraints inherent in this system the yield is fairly high. The absolute amount of light absorbed is uncertain for several reasons. Each treatment was based on the assumption that the wafers were infinitely thick. The wafers used in the infrared analysis were nearly "infinitely" thick, but the variation of quantum yield with thickness is evidence that some light was transmitted. This was shown by the apparent increase in the quantum yield for the pseudo-zeroth order and attenuation due to product models where increasing product concentration per square centimeter gave larger apparent quantum yields while the first order approximation showed only a slight decrease as the initial total concentraton and thickness increased.

The assumption of infinite thickness was valid for the diffuse reflectance measurements. Unfortunately, the reflectance study suffers from the fact that the incident light intensity (for both reaction and reflection) could not be filtered, thus the formation of product may be due to the absorption of several different energy bands. Further, the calibration of the unfiltered source probably resulted in a higher apparent value for the intensity since ferrioxalate is sensitive to all light radiation between 250 nm and 500 nm. This problem may not be as serious as first imagined, however, since $[Rh(NH_3)_5I]^{2+}$ also has a considerable (though somewhat smaller) quantum yield[17] between 250-400 nm.

Other factors incorporated into this average apparent quantum yield are radiative and nonradiative deactivation processes on the molecular level. It is well established[65-66] that the excited state leading to photoaquation has been assigned to a d-d triplet, the same state which is responsible for phosphorescence. Phosphorescence studies in methanol water glasses at 77 K have been reported[65,66] and have been compared[66] with proposed non-radiative processes both at the above temperature and in solution at 298 K. For that luminescence study performed at room temperature,[67] it was observed that the luminescence lifetime was three orders of magnitude shorter at room temperature than at 77 K. The photoreaction which is known to occur at 298 K was not observed at 77 K. The luminescence of adsorbed $[Rh(NH_3)_5I]^{2+}$ was not measured here but its lifetime would be expected to be relatively short, by analogy.

A comparison of the perdeutero and perprotio $[RhA_5X]^{2+}$ complexes, where X is Cl^- or Br^- at both 298 K and 77 K showed that the lifetime of the excited state was longer for the deutrated complexes, and in the study performed at 298 K it was observed that the quantum yields for the photoreaction was directly correlated to the excited lifetime. It appears from this isotope study that one of the main non-radiative deactivation pathways is through weak coupling of N-H stretching vibrations.

In 1972, Kelly and Endicott[16] found no variation of the quantum yield of the photoreaction when perdeuterated rhodium complexes were irradiated. Although they acknowledge that non-radiative deactivation occurs through weak coupling of N-H stretching vibrations

at 77 K, they propose a strong coupling mechanism involving metal-ligand vibrations to explain the absence of an isotope effect at 298 K. In any case, non-radiative deexcitation involves intersystem crossing which results in a vibrational excitation followed by thermal relaxation. In the present system the zeolite may act as a heat sink, accepting the vibrational energy as it drains off the relaxing rhodium complex.

It is important to remember that all of these factors may play a role in determining the quantum yield of the adsorbed rhodium complex. These factors are difficult to separate, indeed there is still some question as to the nonradiative deactivation pathway for this complex in solution.[66] Nevertheless, it is believed that there will, in general, be a decrease in quantum yield for reactions in the zeolite as compared with those in solution.

It is apparent from the present study that the pseudo zero order approximation is only useful for small conversion which is precisely the region where the error in measuring the product concentration is large. The first order approximation is more useful in that results obtained at higher conversion can be used to obtain a more accurate measure of the concentration of product. Unfortunately, it is at higher conversion where source attenuation by the product becomes important. Source attenuation due to product absorption is adequately accounted for by assuming that the transmission of light through the product skin decreases as e^{-kx}. The constant k is considered to be a combination of scattering and product absorption factors. As expected the value of k' determined was relatively constant (Table VI).

Table VI. Quantum Yield and Attenuation Constant for $[Rh(NH_3)_5I]^{2+}$ in Solid Zeolite Wafers

Thickness um	ϕ	k'
32	0.28	-6.09×10^5
37	0.32	-6.04×10^5
40	0.36	-2.73×10^5
38[a]	0.29	-5.33×10^5
		$\overline{k'} = -5.05 \times 10^5$ [b]

All wafers were hydrated except a, which was dehydrated as described in the text. b, Average value.

It should be remembered, however, that this treatment is an empirical one.

Similarly, the Kubelka-Monk theory used to derive the quantum yield from reflectance data (eq 54) is also an empirical method. The scattering coefficient as defined by the Kubelka-Monk theory is not really separable from the other parameters; hence, the exact influence of scattering is obtained via a slightly different route. The scattering is related, in a very real sense to the refractive index of the media as explained in the particle theory with regards to reflectance phenomena (see theory section).

Despite large infrared scattering due to the zeolite support for wafers which are infinitely thick ($\geq$60 μm), the use of infrared spectroscopy, especially in conjunction with visible, transmission and reflectance spectroscopies, will probably receive more attention in the future since it offers several advantages. These include the ability to detect very small amounts of reactants and products (on the order of 0.02 μmole and, in many instances to identify the reactants and products. Transmission infrared also offers the advantage of being able to observe the reaction in the interior of the wafer as well as at the surface. This allowed for the quantitative determination of product.

One of the most appealing methods recently proposed to alleviate the problem of scattering for the purpose of studying photochemical reactions is based on immersing the solid in a liquid of similar refractive index.

Although the immersion technique is not new to spectroscopy,[26] it probably was not until 1979 when some of the first quantitative analyses were done.[21] Thus, if an inert solvent with a refractive index similar to that of the zeolite is introduced the quantum yield may be more accurately determined using infrared and visible transmission data. Many organic compounds fall within this range.[68] If an appropriate solvent were found, many of the assumptions and approximations needed to account for scattering effects might be eliminated thus further work might seriously consider the use of some liquid.

In a hypothetical example one may consider a zeolite catalyst which was capable of photolyzing water but in which conversion was low due to light scattering. If the solid could be immersed in a solution of similar refractive index the scattering problem would be eliminated. One possible solution would be an aqueous solution of sucrose (84-85%) which has a refractive index which is the same as many naturally occurring zeolites, ca. 1.5. This type of solution would also be a constant source of the reactant, water which could easily be replaced as the reaction progressed.

This is not to suggest that a sucrose solution would be the answer to the scattering problem. Still the idea of using some sort of aqueous/solute system is intriguing.

CONCLUSION

Despite the theories thus far advanced to deal with the photophysical and photochemical properties for the solid state, the determination of an absolute quantum yield of solids remains difficult. The most significant problem is light scattering due to the relative opacity of the solid or in the present case of the support. This scattering depends on the index of refraction of the solid, the particle size, and the molar absorptivity of the absorbing moiety. Another problem is due to the rigidity of the support (or solid) which prevents or impedes the diffusion of the absorbing (reactive) species. This causes a concentration gradient which varies with depth into the sample. If the product absorbs significantly in the same region as the reactant, this will lead to an inner filter effect.

In supported systems, non-radiative deactivation may involve the use of the support as a potential heat sink. Finally, if the chromophore is adsorbed on two or more different sites, the quantum yield could be dependent on the nature of these sites.

It is important to keep in mind the assumptions and approximations that permitted an apparent quantum yield to be determined. These include: a) the powdered sample must be considered infinitly thick; b) the particle size should be relatively large with respect to the wavelength of the incident radiation; c) the particles must be considered ideal diffusers (i.e., they scatter light in every direction with equal intensity; d) adjacent particles are considered to have similar reflectance values during the reaction; e) the index of refraction remains constant during the reaction; and f) for adsorbed

species the chromophore is not attached to more than one type of site.

The methods which appear to best describe the system are based on the attenuation due to product model, the continuous medium model (Kubelka-Monk theory) and the particle model. The quantum yield obtained in these cases, 0.30 is only ~30% of that obtained in solution. Since approximations were made in every treatment, a less precise but possibly more accurate quantum yield representative of all these treatments would be 0.26±0.06. Nevertheless, this value is sufficient to prove that photochemical reactions can occur within the zeolite at a measurable rate.

APPENDIX A

The remission function may be derived as follows. The necessary equations include:

$$dI/dx = -(k'+s)I+sJ \tag{1A}$$

$$dJ/dx = (k'+s)J-sI \tag{2A}$$

and

$$R = J/I \tag{3A}$$

the derivative of eq 3A with respect to x is:

$$dR/dx = \frac{I(dJ/dx) - J(dI/dx)}{I^2} \tag{4A}$$

Substituting equations 1A and 2A into 4A yields:

$$dR/dx = \frac{I[(k'+s)J-sI] - J[-(k'+s)I+sJ]}{I^2} \tag{5A}$$

Performing the division and collecting the terms gives

$$dR/dx = \frac{2(k'+s)J}{I} - s - s\frac{J^2}{I^2} \tag{6A}$$

this derivative will go to zero as x goes to , and after recalling eq 3A one gets:

$$2(k'+s)R - s - R^2 = 0 \tag{7A}$$

The solution proceeds from here as follows:

$$2k'R = s-2sR+sR^2$$

$$sk'R = s(1-2R+R^2)$$

$$\frac{k'}{s} = \frac{(I-R)^2}{2R} = f \tag{8A}$$

where 8A is the remission function.

APPENDIX B

KJELDAHL DETERMINATION OF AMMONIUM ION

This method is useful in general for the determination of nitrogen in the form NH_3 or NH_4^+. Compounds containing oxidized forms of nitrogen must first be reduced if this type of analysis is to be performed. Bound amine or coordinated ammine ligands must first be liberated by the action of a strong acid. In the present case the nitrogen is already present as NH_4^+ and the method proceeds as follows.[69,70]

1) Set up a distillation apparatus as shown (Figure 19).

2) Place ~50 ml of 0.4 M H_3BO_3 (an excess) in the receiving flask and make sure that the tip of the adapter reaches below the surface of the solution.

3) Place 0.5 to 0.7 g of zeolite (corresponding to 0.9% wt NH_4^+) in the 300 mL round bottom flask. Add 75 mL H_2O and a stir bar.

4) Connect distillation apparatus together making sure it is leak free.

5) Place a saturated solution of NaOH 75 mL (42 g/100 mL) in the addition funnel.

6) Stir and heat until solution reaches a gentle boil. Read steps 7 through 11 before proceeding further.

7) Begin dropping in concentrated NaOH; the ammonia formed will react with the H_3BO_3 in solution and begin to draw this solution up the condenser.

8) Adjust the bleeder clamp to keep the boric acid solution only in the adapter. Avoid boiling caused by too much suction.

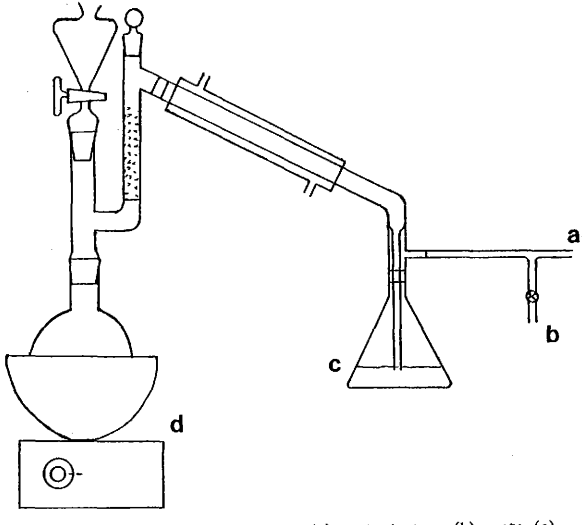

Figure 19. Distillation apparatus: (a) to Aspirator; (b) vent; (c) glass tubing should extend into the boric acid solution; (d) magnetic stirrer/heating mantle.

9. After ~70 mL of NaOH has been added close off the addition funnel and allow the reaction to continue.

10. As NH_3 formation drops, the pressure of the system will increase and the amount of suction may be reduced gradually until the liquid (water) begins to distill over.

11. At this point the aspiration should be small or in some cases unnecessary.

12. Distill ~30 ml of water to collect all the ammonia that may have dissolved in the water vapor clinging to the walls of the condenser. (During this time the zeolite should dissolve almost completely).

13. Open the addition funnel to release the pressure on the "pot" side first, then disconnect the aspirator and turn off the heater.

14. Disconnect the boric acid solution flask and rinse off the adaptor with distilled deionized water. Collect this wash in the boric acid flask.

Titration

15. Add 10 drops of mixed indicator methyl red bromocresol green (0.1% of each in 50% ethanol/water solution) into the collection flask. The solution should be blue-green.

16. Titrate with standard 0.01 M hydrochloric acid to a pale pink endpoint.

17. Calculate the amount of ammonium ion in the zeolite.

18. Repeat with a blank.

REFERENCES AND NOTES

(1) (a) Wrighton, M. S. Chem. & Eng. News 1979, Sept. 3, 29.
(b) Holmes, J. J. Chemtech. 1980, Aug., 514

(2) Sprintschnik, G.; Sprintschnik, H. W.; Kirsch, P. P.; Whitten, D. G. J. Am. Chem. Soc. 1976, 98, 2337

(3) Creutz, C.; Sutin, N. Proc. Nat. Acad. Sci. USA 1975, 72, 2858.

(4) Balzani, V.; Moggi, L.; Manfrin, M. F.; Bolletta, F.; Gleria, M. Science 1975, 189, 852.

(5) Lehn, J. M.; Sauvage, J. P. Nouveau J. de Chemie 1978, 1, 449.

(6) Bockris, J. O'M. "Energy, the Solar Hydrogen Alternative," J. Wiley and Sons, Inc.: New York, 1975; p. 14.

(7) (a) Venuto, P. B. Adv. Chem. Ser. 1971, 102, 260.
(b) Lombardo, E. A.; Sill, G. A.; Hall, W. K. Adv. Chem. Ser. 1971, 102, 346.

(8) Barrer, R. M. "Zeolites and Clay Minerals as Sorbents and Molecular Sieves"; Acad. Press: New York, 1978; p. 14.

(9) (a) Adamson, A. W.; Fleischauer, P. D. "Concepts of Inorganic Photochemistry"; J. Wiley and Sons, Inc.: New York, 1975; p. 381.

(10) (a) Adamson, A. W.; Fleischauer, P. D. "Concepts of Inorganic Photochemistry"; J. Wiley and Sons, Inc.: New York, 1975; p. 145.
(b) Balzani, V.; Carassite V. "Photochemistry of Coordination Compounds"; Acad. Press: New York, 1970.

(11) Wasgestian, H. F.; Schläfer, H. L. Z. Phys. Chem. (Frankfurt) 1968, 62, 127.

(12) Ricciarí, P.; Schlafer, H. L. Inorg. Chem. 1970, 9, 727.

(13) Adamson, A. W. Discuss. Faraday Soc. 1960, 29, 163.

(14) Adamson, A. W.; Sparer, A. H. J. Am. Chem. Soc. 1958, 80, 3865.

(15) Jørgensen, C. K. Acta Chem. Scand. 1956, 10, 500.

(16) Kelly, T. L.; Endicott, J. F. J. Phys. Chem. 1972, 76, 1937.

(17) Kelly, T. L.; Endicott, J. F. J. Am. Chem. Soc. 1972, 94, 1797.

(18) Calvert, J. G.; Pitts, J. N. "Photochemistry"; J. Wiley and Sons, Inc.: New York, 1966; p. 587.

(19) Ibid, p. 795.

(20) Rohatgi-Mukherjee, K. K. "Fundamentals of Photochemistry"; J. Wiley and Sons, Inc.: New York, 1978; pp. 212-213.

(21) Fassler, D.; Gade, R.; Guenther, W. J. Photochem. 1980, 13, 49

(22) Anpo, M.; Kubokawa, Y. Bull. Chem. Soc. Jpn 1977, 50, 31.

(23) Otsuka, K.; Fukaya, M.; Morikawa, A. Bull. Chem. Soc. Jpn 1978, 51, 367.

(24) Otsuka, K.; Eshima, K.; Morikawa, A. Bull. Chem. Soc. Jpn 1977, 50, 531.

(25) Nicholls, C. H.; Leermakers, P. A. Adv. Photochem. 1971, 8, 315.

(26) Robin, M.; Trublood, K. N. J. Am. Chem. Soc. 1957, 79, 5138.

(27) Simmons, E. L.; Wendlandt, W. W. Coord. Chem. Rev. 1971, 7, 11.

(28) Simmons, E. L.; Wendlandt, W. W. Anal. Chim. Acta 1971, 53, 81.

(29) Simmons, E. L. Opt. Acta 1971, 18, 59.

(30) Simmons, E. L. Appl. Opt. 1976, 15, 951.

(31) Simmons, E. L.; Wendlandt, W. W. J. Phys. Chem. 1975, 79, 1158.

(32) Simmons, E. L. J. Phys. Chem. 1976, 80, 1592.

(33) Simmons, E. L. Coord. Chem. Rev. 1974, 14, 181.

(34) Simmons, E. L. J. Chem. Phys. 1976, 65, 5357.

(35) Spencer, H. E. J. Phys. Chem. 1969, 73, 2316.

(36) Simmons, E. L. J. Phys. Chem. 1974, 78, 1265.

(37) Simmons, E. L. J. Phys. Chem. 1971, 75, 588.

(38) Simmons, E. J. J. Chem. Phys. 1977, 66, 1413.

(39) Spencer, H. E.; Schmidt, M. W. J. Phys. Chem. 1970, 74, 3472.

(40) Spencer, H. E.; Schmidt, M. W. J. Phys. Chem. 1971, 75, 2986.

(41) Pitts, J. N.; Wan, J.K.S.; Schuck, E. A. J. Am. Chem. Soc. 1964, 86, 3606.

(42) Ahmed, A.; Gallei, E. Appl. Spec. 1974, 28, 430.

(43) In this work concentrations of 2×10^{-8} mole/cm^2 were common.

(44) Simmons, E. L. Appl. Opt. 1975, 14, 1380.

(45) Melamed, N. T. J. Appl. Phys. 1963, 34, 560.

(46) Addison, A. W.; Dawson, K.; Gillard, R. D.; Heaton, B. T.; Shaw, H. J. Chem. Soc. Dalton Trans. 1972, 589.

(47) Jörgensen, S. M. J. Prak. Chem. 1883, 27, 433.

(48) This was based on stoichiometric considerations and not as excess as indicated by Jörgensen.[47]

(49) Jørgensen, C. K. Acta Chem. Scand. 1956, 10, 500.

(50) Bushnell, G. W.; Lalor, G. C.; Moelwyn-Hughes, E. A. J. Chem. Soc. A 1966, 717.

(51) Suspension is used here, not in the true sense, but to signify a stirred solid/liquid media.

(52) This was not isolated, but its purity was deduced from the large yield (~98%) and high purity (by UV-Vis. spectra) of the resulting perchlorate.

(53) Breck, D. W. "Zeolite Molecular Sieves"; J. Wiley and Sons, Inc.: New York, 1974; p. 177.

(54) In comparing numbers of ions per unit cell here, the hydrated unit cell composition is assumed to be $Na_{56}^{I}(AlO_2)_{56}(SiO_2)_{136}^{I} \cdot 250H_2O$ as described in Reference 53.

(55) Gordon, A. J.; Ford, R. A. "Chemists Companion", J. Wiley and sons, Inc.: New York, 1972, p. 361.

(56) (a) Morov, S. L. "Handbook of Photochemistry", Marcel Dekker, Inc.: New York, 1973; p. 117.

(b) Hatchard, C. G.; Parker, C. A. Proc. Roy. Soc. A. 1956, 235, 518.

(57) Fortune, W. B.; Mellon, M. G. Indus. & Eng. Chem., Anal. Ed. 1938, 10, 60.

(58) Krauss, H. L.; Stack, H. Z. Anorg. Allg. Chem. 1968, 366, 34.

(59) Little, L. H. "I. R. Spectra of Adsorbed Species"; Acad. Press: New York, 1966, p. 366.

(60) Nakamoto, K. "Infrared Spectra of Inorganic and Coordination Compounds", 2nd ed.; J. Wiley and Sons, Inc.: New York, 1970; p. 155.

(61) Szymanski, H. A.; Stamires, D. N.; Lynch, G. R. J. Opt. Soc. Am. 1960, 50, 1323.

(62) Weast, R. C. ed., "CRC Handbook of Chemistry and Physics", 56th ed.; CRC Press: Cleveland, 1975; p. E-196.

(63) Hornbeck, R. W. "Numerical Methods"; Quantum Publishers, Inc.: New York, 1975, p. 121ff.

(64) Wilkins, R. G. "The Study of Kinetics and Mechanisms of Reactions of Transition Metal Complexes", Allyn and Bacon, Inc: Boston, 1974, p. 143.

(65) Thomas, T. R.; Crosby, G. A. J. Mol. Spec. 1971, 38, 118.

(66) Thomas, T. R.; Watts, R. J.; Crosby, G. A. J. Chem. Phys. 1973, 59, 2123.

(67) Bergkamp, M. A.; Watts, R. J.; Ford, P. C.; Brannon, J.; Magde, D. Chem. Phys. Lett. 1978, 59, 125.

(68) Weast, R. C. ed., "CRC Handbook of Chemistry and Physics", 56th ed.; CRC Press: Cleveland, 1975; p. E-221.

(69) Pierce, W. C.; Haenisch, E. L.; Sawyer, D. T. "Quantitative Analysis", 4th ed.; J. Wiley and Sons, Inc., 1958; p. 257.

(70) Fritz, J. S.; Schenk, G. L. "Quantitative Analytical Chemistry", 2nd ed.; Allyn and Bacon, Inc: Boston, 1969; p. 187.

VITA

Michael Joseph Camara was born on March 20, 1955, in Mineola, New York to Mr. and Mrs. Antonio E. Camara. He attended elementary and junior high school in Hicksville, New York and completed his high school education at Hicksville High School in June, 1973. In September, 1973, he attended Fordham University, Bronx, New York and recieved his B. S. degree in May, 1977. In September of that same year he began his graduate study at Texas A&M University.

The author's permanent address is 46 West Cherry Street, Hicksville, New York.

The typist for this thesis was Irene Casimiro.